

Origin of the Heavy Fermion Behavior in $\text{Ca}_{2-x}\text{Sr}_x\text{RuO}_4$: Roles of Coulomb Interaction and the Rotation of RuO_6 octahedra

Naoya Arakawa* and Masao Ogata

Department of Physics, The University of Tokyo, Tokyo 113-0033, Japan

(Dated: June 12, 2018)

We study the electronic states for $\text{Ca}_{2-x}\text{Sr}_x\text{RuO}_4$ in $0.5 \leq x \leq 2$ within the Gutzwiller approximation (GA) on the basis of the three-orbital Hubbard model for the Ru t_{2g} orbitals. The main effects of the Ca-substitution are taken into account as the changes of the dp hybridizations between the Ru $4d$ and O $2p$ orbitals. Using the numerical minimization of the energy obtained in the GA, we obtain the renormalization factor (RF) of the kinetic energy and total RF, which estimates the inverse of the mass enhancement, for three cases with the effective models of $x = 2$ and 0.5 and a special model. We find that the inverse of the total RF becomes the largest for the case of $x = 0.5$, and that the van Hove singularity, which is located on (below) the Fermi level for the special model (the effective model of $x = 0.5$), plays a secondary role in enhancing the effective mass. Our calculation suggests that the heavy fermion behavior around $x = 0.5$ comes from the cooperative effects between moderately strong Coulomb interaction compared to the total bandwidth and the modification of the electronic structures due to the rotation of RuO_6 octahedra (i.e., the variation of the $dp\pi$ hybridizations and the downward shift for the d_{xy} orbital). We propose that moderately strong electron correlation and the orbital-dependent modifications of the electronic structures due to the lattice distortions play important roles in the electronic states for $\text{Ca}_{2-x}\text{Sr}_x\text{RuO}_4$.

PACS numbers: 71.27.+a, 74.70.Pq,

I. INTRODUCTION

Strongly correlated electron systems with orbital degrees of freedom have attracted much interests due to a diversity of phenomena, e.g., a structure-sensitive superconducting transition temperature,¹ a colossal magnetoresistance,^{2,3} and an orbital ordering and the corresponding collective excitations.^{4,5} Among them, the layered perovskite $\text{Ca}_{2-x}\text{Sr}_x\text{RuO}_4$ has rich ground states,^{6,7} in which the Ru $4d$ orbitals play important roles in determining the electronic states.

In $\text{Ca}_{2-x}\text{Sr}_x\text{RuO}_4$, substitution of Ca^{2+} for Sr^{2+} causes three kinds of lattice distortions, i.e., rotation, tilting, and flattening, which affect the electronic structures.^{7,8} Starting from $x = 2$ (i.e., Sr_2RuO_4), which is a spin-triplet superconductor,^{9–11} the ground state changes from the spin-triplet superconductor to a paramagnetic (PM) metal in the range of $0.5 \leq x < 2$. In particular, in the range of $0.5 \leq x < 1.5$, the Ca substitution induces a rotation of RuO_6 octahedra around the c axis (see Fig. 1), while the crystalline structure remains tetragonal with a unit cell doubled. Except the vicinity of $x = 2$, the spin susceptibility behaves like the Curie-Weiss type with a Curie constant corresponding to nearly $S = 1/2$, and the Weiss temperature reaches nearly zero at $x = 0.5$.⁶ In the range of $0.2 \leq x < 0.5$, there occurs a structural transition from tetragonal phase to orthorhombic phase at low temperatures, and the Ca substitution induces the tilting of RuO_6 octahedra around a non-symmetric axis in the basal plane. Also, in this range, the spin susceptibility has a peak at some temperature, and the ground state becomes an antiferromagnetically correlated metal.⁷ In the range of $0 \leq x < 0.2$, a flattening of RuO_6 octahedra along the c axis is induced

and there is a first-order metal-insulator transition: the ground state becomes the antiferromagnetic insulator.¹²

Most surprisingly, the coefficient of the electronic specific heat, γ_e , at low temperatures becomes large around $x = 0.5$. The largest value of γ_e reaches 255 mJ/mol-Ru K^2 at $x = 0.5$; this value is about 25 times of that obtained in the density-functional calculation for Sr_2RuO_4 within local-density approximation (LDA).¹³ A similar mass enhancement has been observed in the optical conductivity measurement by using the extended Drude model.¹⁴ In addition, the spin susceptibility and Hall coefficient measured by applying the magnetic field perpendicular to ab plane show peak structures at $T^* \sim 10$ K for $x = 0.3$,¹⁵ which are similar to those obtained for UPt_3 .¹⁶ These experimental results indicate a formation of heavy fermions (HFs) around $x = 0.5$.

Although there have been extensive theoretical works, the origin of this HF behavior has not been clarified yet. Some studies^{17,18} based on the dynamical mean-field theory (DMFT) have proposed that the HF behavior results from the orbital-selective Mott transition (OSMT) for the d_{xz} and d_{yz} orbitals; the OSMT is defined as a partial disappearance of quasiparticles only for some of the conducting bands. However, this contradicts with another DMFT calculation¹⁹ which has used a realistic model of $\text{Ca}_{2-x}\text{Sr}_x\text{RuO}_4$ in $0.5 \leq x \leq 2$: the OSMT does not appear.

The OSMT for the d_{xz} and d_{yz} orbitals also contradicts with several experiments in $\text{Ca}_{2-x}\text{Sr}_x\text{RuO}_4$ around $x = 0.5$. The angle-resolved photoemission spectroscopy (ARPES) measurement²⁰ for $x = 0.5$ and 2 has shown that the Ca substitution does not modify the topologies of the Fermi surfaces (FSs) for the d_{xz} and d_{yz} orbitals. This result is inconsistent with the proposal of the OSMT

since the partial Mott gap should drastically affect the topologies of the FSs. In addition, the optical conductivity measurement¹⁴ for $\text{Ca}_{2-x}\text{Sr}_x\text{RuO}_4$ in $0.06 \leq x \leq 2$ has found that the Drude weights depend weakly on the Ca concentration. This is consistent with the ARPES measurement since the latter shows a small change of the FS from that for Sr_2RuO_4 . Note that the FS for the d_{xy} orbital changes from an electron pocket for $x = 2$ to a hole pocket for $x = 0.5$.

The aim of this paper is to discuss the qualitative origin of the HF behavior in particular near $x = 0.5$ for $\text{Ca}_{2-x}\text{Sr}_x\text{RuO}_4$. We study the electronic states for $0.5 \leq x \leq 2$ within the Gutzwiller approximation (GA) on the basis of the three-orbital Hubbard model for the Ru t_{2g} orbitals (i.e., d_{xz} , d_{yz} , and d_{xy} orbitals). We assume that the Ca substitution affects the electronic structures mainly by the changes of the dp hybridizations between the Ru $4d$ and O $2p$ orbitals. Actually, the density-functional calculation within the LDA has found that the rotation of RuO_6 octahedra affects the electronic structures for $\text{Ca}_{2-x}\text{Sr}_x\text{RuO}_4$ in $0.5 \leq x \leq 2$.²¹ The GA is used to include the effects of electron correlation non-perturbatively, in which the effects lead to the renormalization of the kinetic energy.^{22–26}

Using the numerical minimization of the energy obtained in the GA, we obtain the renormalization factor (RF) of the kinetic energy for the Ru t_{2g} orbitals and total RF, which estimates the inverse of the mass enhancement, for the effective models of $x = 2$ and 0.5 . We find that the difference between the total RFs for the cases of $x = 2$ and 0.5 becomes large as the intraorbital Coulomb interaction is strong; this arises from the criticality approaching the usual Mott transition, where the occupation numbers for the $d_{xz/yz}$ and d_{xy} orbitals are 1 and 2, respectively. In addition, we analyze a special model in which the van Hove singularity (vHs) for the d_{xy} orbital is located on the Fermi level. We find that the total RF is smaller for the effective model of $x = 0.5$ than that for the special model; the vHs plays a secondary role in enhancing the effective mass. These results are consistent with the experimentally observed tendency of the effective mass in $0.5 \leq x \leq 2$, i.e., monotonic increase of γ_e towards $x = 0.5$.¹³ Our calculation suggests that the HF behavior around $x = 0.5$ comes from the cooperative effects between moderately strong Coulomb interaction compared with the total bandwidth and the significant modification of the electronic structures for the Ru t_{2g} orbitals due to the rotation of RuO_6 octahedra; the latter includes both the variation of the $dp\pi$ hybridizations and the downward shift for the d_{xy} orbital.

The paper is organized as follows. Section II is devoted to the explanations of the method to take account of the main effects of the Ca substitution on the electronic structures in $0.5 \leq x \leq 2$ and the GA for a PM state of the degenerate d_{xz} and d_{yz} orbitals and the d_{xy} orbital. In Sec. III, we show the numerical results of the GA for three cases with the effective models of $x = 2$ and 0.5 and the special model. In Sec. IV, we compare our

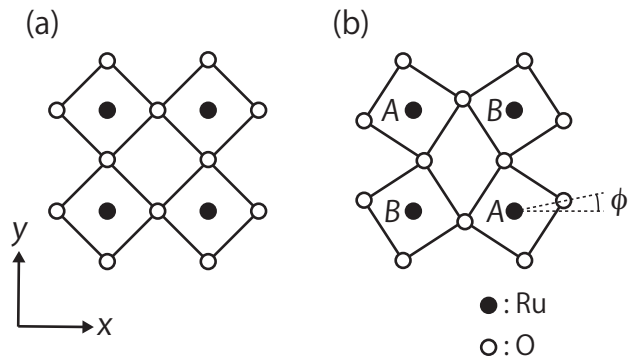


FIG. 1: Schematic pictures of a xy plane of RuO_6 octahedra for (a) $1.5 \leq x \leq 2$ and (b) $0.5 \leq x < 1.5$. Black (white) circles represent Ru (O) ions. ϕ is the angle of the rotation of RuO_6 octahedra. A and B are the indices of two sublattices.

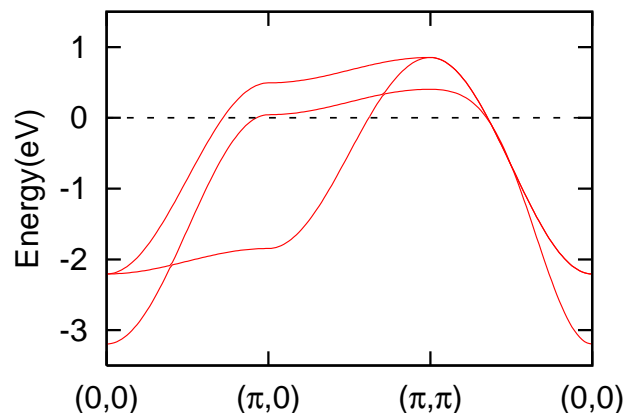


FIG. 2: (Color online) Band structure of the Ru t_{2g} orbitals for the effective model of $x = 2$. The dashed black line represents the chemical potential.

results with previous theoretical studies and remark on the correspondence of our results with experimental results. The paper concludes with a summary of our results in Sec. V.

II. FORMULATION

In the following, we choose the coordinates, x , y , and z , in the directions of the bonds between Ru and O ions at $\phi = 0^\circ$, where ϕ is an angle of the rotation of RuO_6 octahedra [see Fig. 1(b)]. Namely, the coordinates are fixed in the directions of Sr_2RuO_4 with $\phi = 0^\circ$ even for the cases with finite values of ϕ . For convenience, the five Ru $4d$ orbitals, d_{xz} , d_{yz} , d_{xy} , $d_{x^2-y^2}$, and $d_{3z^2-r^2}$, are labeled 1, 2, 3, 4, and 5, respectively.

According to the density-functional calculations^{27,28} for Sr_2RuO_4 within the LDA, the antibonding bands of the Ru t_{2g} and O $2p$ orbitals form the conducting bands in the vicinity of the Fermi level, and the density of states (DOS) near the Fermi level is originated mainly from the

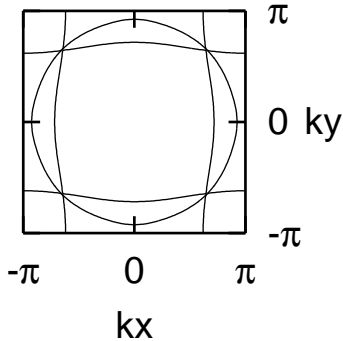


FIG. 3: FSs for the effective model of $x = 2$.

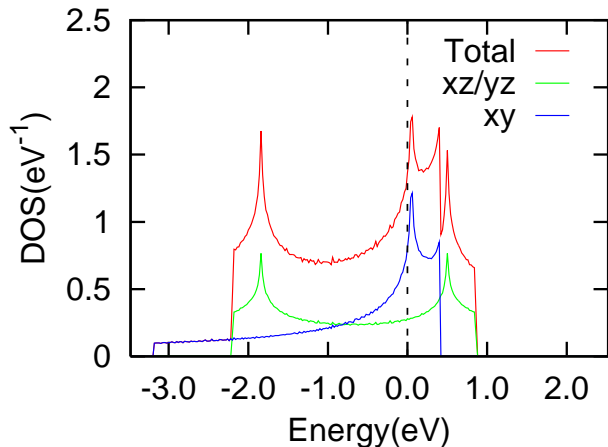


FIG. 4: (Color online) DOS for the effective model of $x = 2$. The dashed black line represents the chemical potential.

Ru t_{2g} orbitals. The partial density of states (pDOS) for the O $2p$ orbitals is roughly a quarter of those for the Ru t_{2g} orbitals. In addition, the x-ray measurements in $\text{Ca}_{2-x}\text{Sr}_x\text{RuO}_4$ have shown that the crystalline-electric-field (CEF) energy between the Ru e_g orbitals and Ru t_{2g} orbitals is of the order of 1 eV.^{29,30} Thus, the Ru t_{2g} orbitals play main roles in determining the electronic states for $\text{Ca}_{2-x}\text{Sr}_x\text{RuO}_4$ at low temperatures. In Sec. IV, we remark on the roles of the Ru e_g and O $2p$ orbitals.

In order to study the electronic states, we use the three-orbital Hubbard model for the Ru t_{2g} orbitals. The unit cell contains one Ru atom for $1.5 \leq x \leq 2$, while it contains two Ru atoms for $0.5 \leq x < 1.5$ due to the rotation of RuO_6 octahedra. As shown in Fig. 1 (b), the directions of the rotation alternate in the two-dimensional square lattice, leading to a unit cell doubled.

The noninteracting Hamiltonian is

$$\hat{H}_0 = - \sum_{i,j} \sum_{a,b=1}^3 \sum_{\sigma} (t_{ab}^{i,j}(\phi) \hat{c}_{ia\sigma}^{\dagger} \hat{c}_{jb\sigma} + \text{H.c.}) - \mu \sum_i \sum_{a=1}^3 \hat{n}_{ia}, \quad (1)$$

where $\hat{c}_{ia\sigma}^{\dagger}$ ($\hat{c}_{ia\sigma}$) is the creation (annihilation) operator that creates (annihilates) an electron in t_{2g} orbital

$a (= 1, 2, 3)$ with spin $\sigma (= \uparrow, \downarrow)$ at site i , $\hat{n}_{ia} = \sum_{\sigma} \hat{n}_{ia\sigma} = \sum_{\sigma} \hat{c}_{ia\sigma}^{\dagger} \hat{c}_{ia\sigma}$, and H.c. means the Hermitian conjugate. Here, $t_{ab}^{i,j}(\phi)$ and μ denote the values of in-plane hopping integrals at an angle ϕ and the chemical potential, respectively. μ is determined so as to satisfy $n_e = 4$ with n_e being the total occupation number for the Ru t_{2g} orbitals. For simplicity, we neglect the effect of the spin-orbit interaction on the electronic structures; the validity is addressed in Sec. IV.

The hopping integrals for Sr_2RuO_4 with $\phi = 0^\circ$ are determined³¹ so as to reproduce the FSs obtained in the de Haas-van Alphen effect:³² the dispersions are given by

$$\epsilon_{11}(\mathbf{k}, 0^\circ) = -2t_1 \cos k_x - 2t_2 \cos k_y - \mu, \quad (2)$$

$$\epsilon_{22}(\mathbf{k}, 0^\circ) = -2t_2 \cos k_x - 2t_1 \cos k_y - \mu, \quad (3)$$

$$\epsilon_{33}(\mathbf{k}, 0^\circ) = -2t_3(\cos k_x + \cos k_y) - 4t_4 \cos k_x \cos k_y - \mu, \quad (4)$$

$$\epsilon_{ab}(\mathbf{k}, 0^\circ) = 0 \quad \text{for } a \neq b, \quad (5)$$

where $t_1/t_3 = 1.5$, $t_2/t_3 = 0.2$, and $t_4/t_3 = 0.4$. In this tight-binding model, we neglect both the weak hybridization between the d_{xz} and d_{yz} orbitals and the difference of the CEF energy between the $d_{xz/yz}$ and d_{xy} orbitals for simplicity.³¹ In this work, we set $t_3 = 0.45$ eV to make W_{tot} about 4 eV. Figures 2–4 show the band structure of the Ru t_{2g} orbitals, the FSs, and the DOS, respectively. In the next section, we describe the dependence of the dispersions on ϕ for $0.5 \leq x < 1.5$.

The interacting Hamiltonian is

$$\begin{aligned} \hat{H}_{\text{int}} = & U \sum_i \sum_a \hat{n}_{ia\uparrow} \hat{n}_{ia\downarrow} + U' \sum_i \sum_{a>b} \hat{n}_{ia} \hat{n}_{ib} \\ & - J_{\text{H}} \sum_i \sum_{a>b} (2\hat{s}_{ia}^z \cdot \hat{s}_{ib}^z + \frac{1}{2}\hat{n}_{ia} \hat{n}_{ib}), \end{aligned} \quad (6)$$

where U , U' , and J_{H} are the intraorbital Coulomb interaction, the interorbital Coulomb interaction, and the Hund's rule coupling; \hat{s}_{ia} is defined as $\hat{s}_{ia} = (1/2) \sum_{\sigma, \sigma'} \hat{c}_{ia\sigma}^{\dagger} \boldsymbol{\sigma}_{\sigma, \sigma'} \hat{c}_{ia\sigma'}$ with $\boldsymbol{\sigma}_{\sigma, \sigma'}$ being the Pauli matrices. In the interacting Hamiltonian, we have neglected both the pair hopping J' and the transverse components of J_{H} for simplicity; the roles of these terms are discussed in Sec. IV. We thus consider the following Hamiltonian in the absence of the rotation of RuO_6 octahedra:

$$\hat{H}_0 + \hat{H}_{\text{int}}. \quad (7)$$

A. Effects of the Ca substitution on the electronic structures in $0.5 \leq x \leq 2$

As described in Sec. I, the Ca substitution induces the rotation of RuO_6 octahedra along the c axis in $0.5 \leq x < 1.5$. In order to take account of effects of the Ca substitution on the electronic structure, we assume that the main effects of the Ca substitution are the changes of the dp hybridizations due to this rotation. As shown in Fig. 1 (b), this rotation changes both the Ru-Ru lengths and the overlap integrals between the Ru $4d$

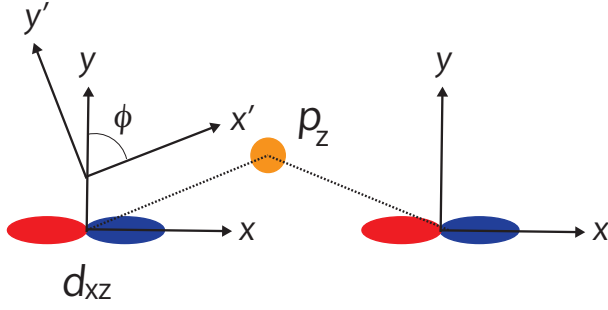


FIG. 5: (Color online) Schematic picture of the in-plane $dp\pi$ hybridization of the Ru d_{xz} orbital to the O p_z orbital in the presence of the rotation of RuO₆ octahedra. x and y (x' and y') are the coordinates in non-rotated (rotated) frame. The difference of a color in the d_{xz} orbital represents that of the sign of the wave function for the d_{xz} orbital.

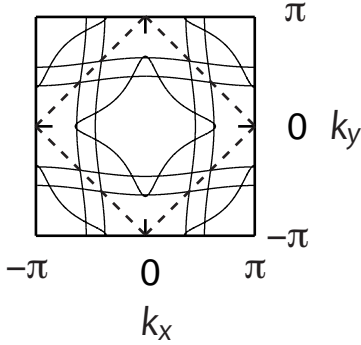


FIG. 6: FSs for the effective model of $x = 0.5$. The dashed line represents the folded Brillouin zone in the presence of the rotation of RuO₆ octahedra.

and O $2p$ orbitals keeping the Ru-O bond lengths constant. The former leads to negligible effects on the electronic structures since the angle dependence of the Ru-Ru lengths is $\cos\phi$, and the latter results in the change of the dp hybridizations linear in ϕ .

We first explain the method to construct the tight-binding model by taking into account the effects of the rotation of RuO₆ octahedra on the electronic structures. As shown in Fig. 5, we can represent the wave functions for the Ru $4d$ and O $2p$ orbitals in the non-rotated frame (x, y, z) by those in the rotated frame (x', y', z'):

$$\begin{aligned}\psi_1(\mathbf{r}) &= \psi_{d_{xz}}(\mathbf{r}) \\ &= \psi_{d_{x'z'}}(\mathbf{r}) \cos\phi - \psi_{d_{y'z'}}(\mathbf{r}) \sin\phi,\end{aligned}\quad (8)$$

$$\begin{aligned}\psi_2(\mathbf{r}) &= \psi_{d_{yz}}(\mathbf{r}) \\ &= \psi_{d_{x'y'}}(\mathbf{r}) \sin\phi + \psi_{d_{y'y'}}(\mathbf{r}) \cos\phi,\end{aligned}\quad (9)$$

$$\begin{aligned}\psi_3(\mathbf{r}) &= \psi_{d_{xy}}(\mathbf{r}) \\ &= \psi_{d_{x'y'}}(\mathbf{r}) \cos 2\phi + \psi_{d_{x'2-y'2}}(\mathbf{r}) \sin 2\phi,\end{aligned}\quad (10)$$

$$\begin{aligned}\psi_4(\mathbf{r}) &= \psi_{d_{x2-y2}}(\mathbf{r}) \\ &= -\psi_{d_{x'y'}}(\mathbf{r}) \sin 2\phi + \psi_{d_{x'2-y'2}}(\mathbf{r}) \cos 2\phi,\end{aligned}\quad (11)$$

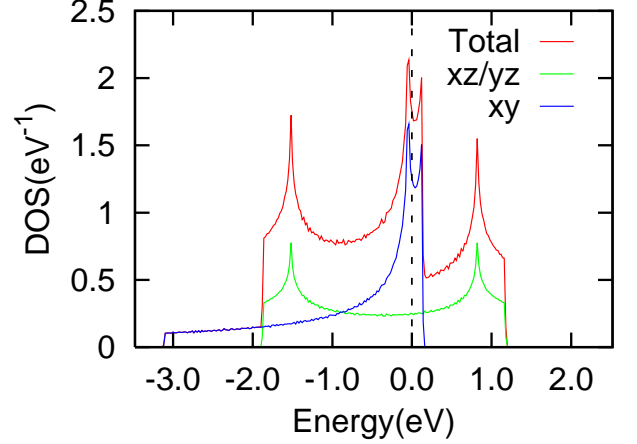


FIG. 7: (Color online) DOS for the effective model of $x = 0.5$. The dashed black line represents the chemical potential.

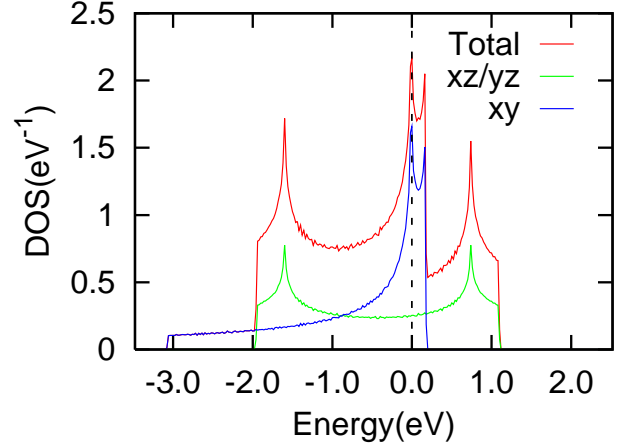


FIG. 8: (Color online) DOS for the special model. The dashed black line represents the chemical potential.

and

$$\psi_{p_x}(\mathbf{r}) = \psi_{p_{x'}}(\mathbf{r}) \cos\phi - \psi_{p_{y'}}(\mathbf{r}) \sin\phi,\quad (12)$$

$$\psi_{p_y}(\mathbf{r}) = \psi_{p_{x'}}(\mathbf{r}) \sin\phi + \psi_{p_{y'}}(\mathbf{r}) \cos\phi,\quad (13)$$

$$\psi_{p_z}(\mathbf{r}) = \psi_{p_{z'}}(\mathbf{r}).\quad (14)$$

The dp hybridizations in the rotated frame are equal to those at $\phi = 0^\circ$ since the Ru-O bond length is unchanged;⁸ we have $V_{d_{x'z'}p_{z'}}(\phi) = V_{1p_z}(0^\circ)$ and so on. The finite dp hybridizations at $\phi = 0^\circ$ are $V_{1p_z}(0^\circ)$, $V_{3p_y}(0^\circ)$, and $V_{4p_x}(0^\circ)$ along the x direction and $V_{2p_z}(0^\circ)$, $V_{3p_x}(0^\circ)$, and $V_{4p_y}(0^\circ)$ along the y direction, respectively. There-

fore, the dp hybridizations at ϕ are given by

$$V_{1p_z}(\phi) = V_{1p_z}(0^\circ) \cos \phi, \quad (15)$$

$$V_{2p_z}(\phi) = V_{1p_z}(0^\circ) \sin \phi, \quad (16)$$

$$V_{3p_x}(\phi) = V_{3p_y}(0^\circ) \sin \phi \cos 2\phi + V_{4p_x}(0^\circ) \cos \phi \sin 2\phi, \quad (17)$$

$$V_{3p_y}(\phi) = V_{3p_y}(0^\circ) \cos \phi \cos 2\phi + V_{4p_x}(0^\circ) \sin \phi \sin 2\phi, \quad (18)$$

in the x direction, and

$$V_{1p_z}(\phi) = -V_{2p_z}(0^\circ) \sin \phi, \quad (19)$$

$$V_{2p_z}(\phi) = V_{2p_z}(0^\circ) \cos \phi, \quad (20)$$

$$V_{3p_x}(\phi) = V_{3p_x}(0^\circ) \cos \phi \cos 2\phi - V_{4p_y}(0^\circ) \sin \phi \sin 2\phi, \quad (21)$$

$$V_{3p_y}(\phi) = V_{3p_x}(0^\circ) \sin \phi \cos 2\phi + V_{4p_y}(0^\circ) \cos \phi \sin 2\phi, \quad (22)$$

in the y direction, respectively. Using the second-order perturbation processes with respect to these dp hybridizations, we obtain the following nearest-neighbor hopping integrals among the Ru t_{2g} orbitals:

$$t_{11}^{AB;x}(\phi) = t_1 \cos^2 \phi, \quad (23)$$

$$t_{12}^{AB;x}(\phi) = -\frac{1}{2}t_1 \sin 2\phi, \quad (24)$$

$$t_{21}^{AB;x}(\phi) = -t_{12}^{AB;x}(\phi), \quad (25)$$

$$t_{22}^{AB;x}(\phi) = t_2 - t_1 \sin^2 \phi, \quad (26)$$

$$t_{33}^{AB;x}(\phi) = t_3 \cos^3 2\phi - t_5 \cos 2\phi \sin^2 2\phi + 2t_6 \cos 2\phi \sin^2 2\phi, \quad (27)$$

in the x direction, and

$$t_{11}^{AB;y}(\phi) = t_2 - t_1 \sin^2 \phi, \quad (28)$$

$$t_{12}^{AB;y}(\phi) = -\frac{1}{2}t_1 \sin 2\phi, \quad (29)$$

$$t_{21}^{AB;y}(\phi) = -t_{12}^{AB;y}(\phi), \quad (30)$$

$$t_{22}^{AB;y}(\phi) = t_1 \cos^2 \phi, \quad (31)$$

$$t_{33}^{AB;y}(\phi) = t_3 \cos^3 2\phi - t_5 \cos 2\phi \sin^2 2\phi + 2t_6 \cos 2\phi \sin^2 2\phi, \quad (32)$$

in the y direction, respectively. Here, the superscripts A and B denote the sublattices, and t_1 , t_2 , t_3 , and t_4 are defined in Eqs. (2)–(4). In deriving Eqs. (23)–(32), we have assumed that t_1 in Eqs. (2) and (3) arises from the second-order perturbation process with respect to the dp hybridization of the Ru d_{xz}/yz orbital to the O $2p_z$ orbital: t_1 is given by

$$t_1 = \frac{V_{1p_z}(0^\circ)^2}{E_1(0^\circ) - E_{p_z}(0^\circ)} = \frac{V_{2p_z}(0^\circ)^2}{E_2(0^\circ) - E_{p_z}(0^\circ)}, \quad (33)$$

where $E_a(\phi)$ and $E_b(\phi)$ are the CEF energies at ϕ for the Ru t_{2g} orbital a and the O $2p$ orbital b , respectively.

For the case with $\phi = 0^\circ$, we have $V_{3p_x}(0^\circ) = V_{3p_y}(0^\circ)$ and $E_{p_x}(0^\circ) = E_{p_y}(0^\circ)$. In the presence of the rotation of RuO₆ octahedra, $E_{p_x}(\phi)$ and $E_{p_y}(\phi)$ can be different in principle; however, we have assumed $E_{p_x}(\phi) = E_{p_y}(\phi)$ in deriving Eqs. (23)–(32) for simplicity. Similarly, t_3 in Eq. (4) is given by

$$t_3 = \frac{V_{3p_y}(0^\circ)^2}{E_3(0^\circ) - E_{p_y}(0^\circ)} = \frac{V_{3p_x}(0^\circ)^2}{E_3(0^\circ) - E_{p_x}(0^\circ)}. \quad (34)$$

In contrast, t_2 in Eqs. (2) and (3) arises from the direct hopping process between the d_{xz}/yz orbitals since there are no hybridizations with the O $2p$ orbitals in between; we have assumed that the rotation of RuO₆ octahedra does not affect t_2 in Eqs. (26) and (28). In Eqs. (27) and (32), t_5 and t_6 are the rotation-induced hopping integrals which are defined as

$$t_5 = \frac{V_{4p_x}(0^\circ)^2}{E_3(0^\circ) - E_{p_x}(\phi)} = \frac{V_{4p_y}(0^\circ)^2}{E_3(0^\circ) - E_{p_y}(\phi)}, \quad (35)$$

$$t_6 = \frac{V_{3p_y}(0^\circ)V_{4p_x}(0^\circ)}{E_3(0^\circ) - E_{p_x}(\phi)} = \frac{V_{3p_x}(0^\circ)V_{4p_y}(0^\circ)}{E_3(0^\circ) - E_{p_y}(\phi)}, \quad (36)$$

respectively. The former arises from the hybridizations of the $d_{x^2-y^2}$ orbital in Eq. (10) with the $p_{x'}$ and $p_{y'}$ orbitals in Eqs. (12) and (13), and the latter arises from the hybridizations of the $d_{x'y'}$ and $d_{x^2-y^2}$ orbitals in Eq. (10) with the $p_{y'}$ and $p_{x'}$ orbitals in Eqs. (12) and (13).

Using these hopping integrals Eqs. (23)–(32), we obtain the noninteracting Hamiltonian in the presence of the rotation of RuO₆ octahedra as follows:

$$\hat{H}_0 = \sum_{\mathbf{k}}' \sum_{a,b=1}^3 \sum_{s,s'=A,B} \sum_{\sigma} \epsilon_{ab}^{ss'}(\mathbf{k}, \phi) \hat{c}_{ksa\sigma}^\dagger \hat{c}_{ks'b\sigma}, \quad (37)$$

where

$$\epsilon_{11}^{AA}(\mathbf{k}, \phi) = \epsilon_{22}^{AA}(\mathbf{k}, \phi) = -\mu, \quad (38)$$

$$\epsilon_{33}^{AA}(\mathbf{k}, \phi) = -4t_4 \cos k_x \cos k_y - \mu, \quad (39)$$

$$\epsilon_{11}^{AB}(\mathbf{k}, \phi) = -2t_{11}^{AB;x}(\phi) \cos k_x - 2t_{11}^{AB;y}(\phi) \cos k_y, \quad (40)$$

$$\epsilon_{12}^{AB}(\mathbf{k}, \phi) = -2t_{12}^{AB;x}(\phi) \cos k_x - 2t_{12}^{AB;y}(\phi) \cos k_y, \quad (41)$$

$$\epsilon_{21}^{AB}(\mathbf{k}, \phi) = -\epsilon_{12}^{AB}(\mathbf{k}, \phi), \quad (42)$$

$$\epsilon_{22}^{AB}(\mathbf{k}, \phi) = -2t_{22}^{AB;x}(\phi) \cos k_x - 2t_{22}^{AB;y}(\phi) \cos k_y, \quad (43)$$

$$\epsilon_{33}^{AB}(\mathbf{k}, \phi) = -2t_{33}^{AB;x}(\phi) \cos k_x - 2t_{33}^{AB;y}(\phi) \cos k_y, \quad (44)$$

$$\epsilon_{ab}^{AA}(\mathbf{k}, \phi) = \epsilon_{ab}^{AB}(\mathbf{k}, \phi) = 0 \quad \text{otherwise}, \quad (45)$$

$$\epsilon_{ab}^{BA}(\mathbf{k}, \phi) = \epsilon_{ab}^{AB}(\mathbf{k}, -\phi). \quad (46)$$

The prime in the summation with respect to \mathbf{k} represents the restriction within the folded Brillouin zone in the presence of the rotation of RuO₆ octahedra. For simplicity, we have neglected the effect of the rotation of

RuO₆ octahedra on the next-nearest-neighbor hopping integrals for the Ru 4*d* orbitals.

The rotation of RuO₆ octahedra also induces the hybridization of the *d_{xy}* orbital to the *d_{x²-y²}* orbital although it is not included in Eqs. (23)–(32). Since the energy level for the *d_{x²-y²}* orbital is higher than that for the *d_{xy}* orbital, this hybridization leads to a downward shift of the *d_{xy}* orbital. This effect is approximately taken into account as the difference of the CEF energy, $\Delta_{t_{2g}}$, between the *d_{xz/yz}* and *d_{xy}* orbitals:

$$\hat{H}_{\text{CEF}} = \frac{\Delta_{t_{2g}}}{3} \sum_i (\hat{n}_{i1} + \hat{n}_{i2} - 2\hat{n}_{i3}). \quad (47)$$

In this work, we use $\Delta_{t_{2g}}$ as a parameter. Combining this term and the noninteracting and interacting Hamiltonians, we consider the following Hamiltonian in the presence of the rotation of RuO₆ octahedra:

$$\hat{H}_0 + \hat{H}_{\text{int}} + \hat{H}_{\text{CEF}}. \quad (48)$$

In order to discuss the electronic state for $x = 0.5$, we set $\phi = 15^\circ$ and $(t_5, t_6, \Delta_{t_{2g}}) = (0, 0, 0.42)$ (eV) so as to reproduce the FSs obtained in the ARPES measurement.²⁰ Figures 6 and 7 represent the FSs and the DOS, respectively. In Fig. 6, the absence of the FS around $\mathbf{k} = (\pi, 0)$ corresponds to the change of the FS for the *d_{xy}* orbital from an electron pocket to a hole pocket. There are three main changes of the electronic structures due to the rotation of RuO₆ octahedra: the reduction of the bandwidth for the *d_{xy}* orbital, the increase of the pDOS for the *d_{xy}* orbital near the Fermi level, and the change of the FS for the *d_{xy}* orbital from an electron pocket to a hole pocket. The bandwidth and pDOS for the *d_{xz/yz}* orbital are little affected. These results are qualitatively consistent with those obtained in the density-functional calculation within the LDA²¹ or local-spin-density approximation.³³ We thus think that the present model is reasonable for the study of the electronic states in Ca_{2-x}Sr_xRuO₄ although the experimental value of ϕ is about 12.8° at $x = 0.5$.⁸

In addition, we study a special model in which the vHs for the *d_{xy}* orbital is located on the Fermi level in order to clarify the role of the vHs in enhancing the effective mass. We use the dispersions in Eqs. (38)–(46) setting $\phi = 15^\circ$ and $(t_5, t_6, \Delta_{t_{2g}}) = (0, 0, 0.3)$ (eV); the difference between this case and the case of $x = 0.5$ is that in the values of $\Delta_{t_{2g}}$. Figure 8 shows the DOS in this case.

B. Gutzwiller approximation

In this section, we explain the GA for a PM state consisting of the degenerate *d_{xz}* and *d_{yz}* orbitals and the *d_{xy}* orbital. Let us define the Gutzwiller-type variational wave function as

$$|\Psi_G\rangle = \prod_j \prod_{l=0}^{63} [1 - (1 - g_l) \hat{P}_{j;l}] |\Psi_0\rangle, \quad (49)$$

where $|\Psi_0\rangle$ is the ground state for \hat{H}_0 , $\hat{P}_{j;l}$ are the projection operators, and g_l are the corresponding variational parameters for the l th configuration. There are $4^3 = 64$ configurations for each site j since we have three orbitals and two kinds of spin degrees of freedom. The variational energy is given by

$$E_{\text{gs}} = \min_{\{g_l\}} \frac{\langle \Psi_G | \hat{H} | \Psi_G \rangle}{\langle \Psi_G | \Psi_G \rangle}, \quad (50)$$

where $\min_{\{g_l\}}$ denotes the optimization with respect to $\{g_l\}$, and \hat{H} is the total Hamiltonian given by Eq. (48).

To calculate the expectation values, we use the GA^{22–26} in which the dependence of the Slater determinants on the configurations is neglected. For example, the square of the Slater determinant, $[\det U_{1\uparrow}(\{\mathbf{r}_{1\uparrow}^{N_{1\uparrow}}\})]^2$, for the electrons in $a = 1$ with $\sigma = \uparrow$ can be approximated as

$$[\det U_{1\uparrow}(\{\mathbf{r}_{1\uparrow}^{N_{1\uparrow}}\})]^2 \xrightarrow{\text{GA}} (n_{1\uparrow}^0)^{N_{1\uparrow}} (1 - n_{1\uparrow}^0)^{L - N_{1\uparrow}}, \quad (51)$$

where $\{\mathbf{r}_{1\uparrow}^{N_{1\uparrow}}\}$ is a set of sites occupied by these electrons, L is the number of sites, $N_{1\uparrow}$ is the number of these electrons, and $n_{1\uparrow}^0$ is defined as an expectation value without the projection operators:

$$n_{1\uparrow}^0 = \frac{1}{L} \sum_j \langle \Psi_0 | \hat{n}_{j1\uparrow} | \Psi_0 \rangle = \frac{1}{L} \sum_j \langle \hat{n}_{j1\uparrow} \rangle_0. \quad (52)$$

Using the GA, we can rewrite the denominator in Eq. (50) as

$$\begin{aligned} \langle \Psi_G | \Psi_G \rangle &= \sum_{\{N_{a\sigma}\}} \sum_{\{\mathbf{r}_{a\sigma}^{N_{a\sigma}}\}} \left[\prod_l g_l^{2\Gamma_l(\{\mathbf{r}_{a\sigma}^{N_{a\sigma}}\})} \right] \\ &\times \prod_{a=1}^3 \prod_{\sigma} [\det U_{a\sigma}(\{\mathbf{r}_{a\sigma}^{N_{a\sigma}}\})]^2 \\ &\xrightarrow{\text{GA}} \sum_{\{N_{a\sigma}\}} \sum_{\{\Gamma_l\}} \left(\prod_l g_l^{2\Gamma_l} \right) \frac{L!}{(\prod_l \Gamma_l!)} P(L; \{N_{a\sigma}\}), \end{aligned} \quad (53)$$

with

$$P(L; \{N_{a\sigma}\}) = \prod_{a=1}^3 \prod_{\sigma} (n_{a\sigma}^0)^{N_{a\sigma}} (1 - n_{a\sigma}^0)^{L - N_{a\sigma}}. \quad (54)$$

Here, $\sum_{\{N_{a\sigma}\}}$ denotes the summation with respect to all the possible values $N_{a\sigma}$ ($a = 1, 2, 3$, $\sigma = \uparrow, \downarrow$), Γ_l is the number of sites with the l th configuration, and the summation $\sum_{\{\Gamma_l\}}$ is taken over all the possible values Γ_l ($l = 0 - 63$) under the constraints

$$\sum_{l=0}^{63} \Gamma_l = L, \quad (55)$$

$$\sum_{l=0}^{63} \sum_{a=1,2} \Gamma_l n_{la\sigma} = \sum_{a=1,2} N_{a\sigma}, \quad (56)$$

$$\sum_{l=0}^{63} \Gamma_l n_{l3\sigma} = N_{3\sigma}, \quad (57)$$

where $n_{l a \sigma}$ is the number of electrons in orbital a with spin σ for the l th configuration; as we shall show, $n_{l a \sigma}$ plays important roles in calculating the expectation values within the GA.

Since the occupation number for each orbital is same in A and B sublattices, we do not need to take care of the sublattices in the GA. In other words, the formulation for a PM state consisting of the t_{2g} orbitals without the sublattice indices is sufficient to calculate the expectation values for a PM state consisting of the t_{2g} orbitals with the sublattice indices.

$(N_{1\sigma} + N_{2\sigma})$ and $N_{3\sigma}$ are conserved quantum numbers although $N_{1\sigma}$ and $N_{2\sigma}$ are not conserved quantum numbers due to the finite hopping integral between the d_{xz} and d_{yz} orbitals. In general, the values of $(N_{1\sigma} + N_{2\sigma})$ and $N_{3\sigma}$ may change in the presence of interactions for a system with orbital degrees of freedom. In the following, however, we assume that these values are equal to those in the absence of the interactions; e.g., for the effective model of $x = 2$, $(N_{1\sigma} + N_{2\sigma})/L = (n_1^0 + n_2^0) = 2.66$, $N_{3\sigma}/L = n_3^0 = 1.33$. In Sec. IV, we address the effect of the variation of the occupation numbers due to electron correlation.

In the thermodynamic limit, we can approximate the summation with respect to Γ_l in Eqs. (53) to their largest terms:

$$\langle \Psi_G | \Psi_G \rangle \xrightarrow{\text{GA}} \left(\prod_l g_l^{2\bar{\Gamma}_l} \right) \frac{L!}{(\prod_l \bar{\Gamma}_l!)} P(L; \{N_{a\sigma}\}), \quad (58)$$

where $\{\bar{\Gamma}_l\}$ is the set of $\{\Gamma_l\}$ that gives the largest term. $\bar{\Gamma}_l$ is given by

$$\bar{\Gamma}_l = L g_l^2 \exp(1 + \lambda_0 + \sum_{a=1}^3 \sum_{\sigma} \lambda_{a\sigma} n_{l a \sigma}), \quad (59)$$

where $(\lambda_0, \{\lambda_{a\sigma}\})$ are the Lagrange multipliers²⁶ determined so as to satisfy the constraints Eqs. (55)–(57) for $\{\bar{\Gamma}_l\}$. For simplicity, we assume that the following relations hold in the thermodynamic limit:

$$\frac{N_{a\uparrow}}{L} = \frac{N_{a\downarrow}}{L}, \quad (60)$$

$$\frac{N_{1\sigma}}{L} = \frac{N_{2\sigma}}{L}. \quad (61)$$

Correspondingly, the Lagrange multipliers satisfy

$$\lambda_{a\uparrow} = \lambda_{a\downarrow}, \quad (62)$$

$$\lambda_{2\sigma} = \lambda_{1\sigma}. \quad (63)$$

Similarly, the expectation values of $\hat{n}_{i a \sigma} \hat{n}_{i b \sigma'}$ and $\hat{c}_{i a \sigma}^\dagger \hat{c}_{j b \sigma}$ can be rewritten within the GA as

$$\begin{aligned} & \langle \Psi_G | \hat{n}_{i a \sigma} \hat{n}_{i b \sigma'} | \Psi_G \rangle \\ & \xrightarrow{\text{GA}} \sum_{l_i} \sum_{\{\Gamma'_l\}} g_{l_i}^2 \langle \hat{P}_{i;l_i} \hat{n}_{i a \sigma} \hat{n}_{i b \sigma'} \hat{P}_{i;l_i} \rangle_0 \left(\prod_l g_l^{2\Gamma'_l} \right) \\ & \times \frac{(L-1)!}{(\prod_l \Gamma'_l!)} P(L-1; \{N'_{a\sigma}\}), \end{aligned} \quad (64)$$

and

$$\begin{aligned} & \langle \Psi_G | \hat{c}_{i a \sigma}^\dagger \hat{c}_{j b \sigma} | \Psi_G \rangle \\ & \xrightarrow{\text{GA}} \sum_{l_i, l_j, l'_i, l'_j} \sum_{\{\Gamma'_l\}} g_{l_i} g_{l_j} g_{l'_i} g_{l'_j} \langle \hat{P}_{i;l_i} \hat{P}_{j;l_j} \hat{c}_{i a \sigma}^\dagger \hat{c}_{j b \sigma} \hat{P}_{i;l'_i} \hat{P}_{j;l'_j} \rangle_0 \\ & \times \left(\prod_l g_l^{2\Gamma'_l} \right) \frac{(L-2)!}{(\prod_l \Gamma'_l!)} P(L-2; \{N''_{a\sigma}\}), \end{aligned} \quad (65)$$

with the constraints

$$\sum_{l=0}^{63} \Gamma'_l = L-1, \quad (66)$$

$$\begin{aligned} \sum_{l=0}^{63} \sum_{a=1,2} \Gamma'_l n_{l a \sigma} &= \sum_{a=1,2} N'_{a\sigma} \\ &= \sum_{a=1,2} (N_{a\sigma} - n_{l_i a \sigma}), \end{aligned} \quad (67)$$

$$\begin{aligned} \sum_{l=0}^{63} \Gamma'_l n_{l 3\sigma} &= N'_{3\sigma} \\ &= N_{3\sigma} - n_{l_i 3\sigma}, \end{aligned} \quad (68)$$

and

$$\sum_{l=0}^{63} \Gamma''_l = L-2, \quad (69)$$

$$\begin{aligned} \sum_{l=0}^{63} \sum_{a=1,2} \Gamma''_l n_{l a \sigma} &= \sum_{a=1,2} N''_{a\sigma} \\ &= \sum_{a=1,2} (N_{a\sigma} - n_{l_i a \sigma} - n_{l_j a \sigma}) \\ &= \sum_{a=1,2} (N_{a\sigma} - n_{l'_i a \sigma} - n_{l'_j a \sigma}), \end{aligned} \quad (70)$$

$$\begin{aligned} \sum_{l=0}^{63} \Gamma''_l n_{l 3\sigma} &= N''_{3\sigma} \\ &= N_{3\sigma} - n_{l_i 3\sigma} - n_{l_j 3\sigma} \\ &= N_{3\sigma} - n_{l'_i 3\sigma} - n_{l'_j 3\sigma}. \end{aligned} \quad (71)$$

Here, the summation with respect to l_i in Eq. (64) is taken for the configurations of site i in which there are at least an electron in orbital a with spin σ and an electron in orbital b with spin σ' . In Eq. (65), l_i and l_j are the configurations of sites i and j after the hopping process $\hat{c}_{i a \sigma}^\dagger \hat{c}_{j b \sigma}$ in which there are no electrons in orbital b with spin σ at site j and there is at least an electron in orbital a with spin σ at site i ; l'_i and l'_j are similar configurations of sites i and j before the hopping process. The prime and double prime in the summations of Eqs. (64) and (65) represent these restrictions.

In the thermodynamic limit, we approximate the summation with respect to Γ'_l in Eq. (64) to their largest terms for each configuration of l_i and the summation with respect to Γ''_l in Eq. (65) to their largest terms for the configurations of l_i , l_j , l'_i , and l'_j . Thus, these

expectation values become

$$\begin{aligned} & \langle \Psi_G | \hat{n}_{ia\sigma} \hat{n}_{ib\sigma'} | \Psi_G \rangle \\ & \xrightarrow{\text{GA}} \sum'_{l_i} g_{l_i}^2 \langle \hat{P}_{i;l_i} \hat{n}_{ia\sigma} \hat{n}_{ib\sigma'} \hat{P}_{i;l_i} \rangle_0 \left(\prod_l g_l^{2\bar{\Gamma}'_l} \right) \\ & \times \frac{(L-1)!}{\left(\prod_l \bar{\Gamma}'_l! \right)} P(L-1; \{N'_{a\sigma}\}), \end{aligned} \quad (72)$$

and

$$\begin{aligned} & \langle \Psi_G | \hat{c}_{ia\sigma}^\dagger \hat{c}_{jb\sigma} | \Psi_G \rangle \\ & \xrightarrow{\text{GA}} \sum''_{l_i, l_j, l'_i, l'_j} g_{l_i} g_{l_j} g_{l'_i} g_{l'_j} \langle \hat{P}_{i;l_i} \hat{P}_{j;l_j} \hat{c}_{ia\sigma}^\dagger \hat{c}_{jb\sigma} \hat{P}_{i;l'_i} \hat{P}_{j;l'_j} \rangle_0 \\ & \times \left(\prod_l g_l^{2\bar{\Gamma}''_l} \right) \frac{(L-2)!}{\left(\prod_l \bar{\Gamma}''_l! \right)} P(L-2; \{N''_{a\sigma}\}), \end{aligned} \quad (73)$$

where $\bar{\Gamma}'_l$ and $\bar{\Gamma}''_l$ are given by

$$\bar{\Gamma}'_l = L g_l^2 \exp(1 + \lambda'_0 + \sum_{a=1}^3 \sum_{\sigma} \lambda'_{a\sigma} n_{la\sigma}), \quad (74)$$

$$\bar{\Gamma}''_l = L g_l^2 \exp(1 + \lambda''_0 + \sum_{a=1}^3 \sum_{\sigma} \lambda''_{a\sigma} n_{la\sigma}), \quad (75)$$

respectively. The Lagrange multipliers, $(\lambda'_0, \{\lambda'_{a\sigma}\})$ and $(\lambda''_0, \{\lambda''_{a\sigma}\})$, are determined so as to satisfy the constraints Eqs. (66)–(68) for $\{\bar{\Gamma}'_l\}$ and Eqs. (69)–(71) for $\{\bar{\Gamma}''_l\}$, respectively. For simplicity, we also assume that the following relations hold in the thermodynamic limit:

$$\frac{N'_{a\uparrow}}{L} = \frac{N'_{a\downarrow}}{L}, \quad (76)$$

$$\frac{N'_{1\sigma}}{L} = \frac{N'_{2\sigma}}{L}, \quad (77)$$

and

$$\frac{N''_{a\uparrow}}{L} = \frac{N''_{a\downarrow}}{L}, \quad (78)$$

$$\frac{N''_{1\sigma}}{L} = \frac{N''_{2\sigma}}{L}. \quad (79)$$

Correspondingly, the Lagrange multipliers satisfy

$$\lambda'_{a\uparrow} = \lambda'_{a\downarrow}, \quad (80)$$

$$\lambda'_{2\sigma} = \lambda'_{1\sigma}, \quad (81)$$

and

$$\lambda''_{a\uparrow} = \lambda''_{a\downarrow}, \quad (82)$$

$$\lambda''_{2\sigma} = \lambda''_{1\sigma}. \quad (83)$$

Using Eqs. (58), (72), and (73), we obtain the normalized expectation values of $\hat{n}_{ia\sigma} \hat{n}_{ib\sigma'}$ and $\hat{c}_{ia\sigma}^\dagger \hat{c}_{jb\sigma}$ within the GA in the thermodynamic limit:

$$\begin{aligned} & \frac{\langle \Psi_G | \hat{n}_{ia\sigma} \hat{n}_{ib\sigma'} | \Psi_G \rangle}{\langle \Psi_G | \Psi_G \rangle} \\ & \xrightarrow{\text{GA}} \frac{1}{L} \sum'_{l_i} g_{l_i}^2 \langle \hat{P}_{i;l_i} \hat{n}_{ia\sigma} \hat{n}_{ib\sigma'} \hat{P}_{i;l_i} \rangle_0 \\ & \times \left(\prod_l g_l^{2\Delta\bar{\Gamma}'_l} \right) \frac{\left(\prod_l \bar{\Gamma}'_l! \right)}{\left(\prod_l \bar{\Gamma}'_l! \right)} \frac{P(L-1; \{N'_{a\sigma}\})}{P(L; \{N_{a\sigma}\})}, \end{aligned} \quad (84)$$

and

$$\begin{aligned} & \frac{\langle \Psi_G | \hat{c}_{ia\sigma}^\dagger \hat{c}_{jb\sigma} | \Psi_G \rangle}{\langle \Psi_G | \Psi_G \rangle} \\ & \xrightarrow{\text{GA}} \frac{1}{L^2} \sum''_{l_i, l_j, l'_i, l'_j} g_{l_i} g_{l_j} g_{l'_i} g_{l'_j} \langle \hat{P}_{i;l_i} \hat{P}_{j;l_j} \hat{c}_{ia\sigma}^\dagger \hat{c}_{jb\sigma} \hat{P}_{i;l'_i} \hat{P}_{j;l'_j} \rangle_0 \\ & \times \left(\prod_l g_l^{2\Delta\bar{\Gamma}''_l} \right) \frac{\left(\prod_l \bar{\Gamma}''_l! \right)}{\left(\prod_l \bar{\Gamma}''_l! \right)} \frac{P(L-2; \{N''_{a\sigma}\})}{P(L; \{N_{a\sigma}\})}, \end{aligned} \quad (85)$$

where $\Delta\bar{\Gamma}'_l$ and $\Delta\bar{\Gamma}''_l$ are defined as $\Delta\bar{\Gamma}'_l = \bar{\Gamma}'_l - \bar{\Gamma}_l$ and $\Delta\bar{\Gamma}''_l = \bar{\Gamma}''_l - \bar{\Gamma}_l$, respectively. From Eqs. (55)–(57) for $\{\bar{\Gamma}_l\}$, Eqs. (66)–(68) for $\{\bar{\Gamma}'_l\}$, and Eqs. (69)–(71) for $\{\bar{\Gamma}''_l\}$, we have the following constraints for $\Delta\bar{\Gamma}'_l$ and $\Delta\bar{\Gamma}''_l$:

$$\sum_{l=0}^{63} \Delta\bar{\Gamma}'_l = -1, \quad (86)$$

$$\sum_{l=0}^{63} \sum_{a=1,2} \Delta\bar{\Gamma}'_l n_{la\sigma} = - \sum_{a=1,2} n_{la\sigma}, \quad (87)$$

$$\sum_{l=0}^{63} \Delta\bar{\Gamma}'_l n_{l3\sigma} = - n_{l3\sigma}, \quad (88)$$

and

$$\sum_{l=0}^{63} \Delta\bar{\Gamma}''_l = -2, \quad (89)$$

$$\begin{aligned} \sum_{l=0}^{63} \sum_{a=1,2} \Delta\bar{\Gamma}''_l n_{la\sigma} &= - \sum_{a=1,2} (n_{la\sigma} + n_{lj a\sigma}) \\ &= - \sum_{a=1,2} (n_{l'_i a\sigma} + n_{l'_j a\sigma}), \end{aligned} \quad (90)$$

$$\begin{aligned} \sum_{l=0}^{63} \Delta\bar{\Gamma}''_l n_{l3\sigma} &= - (n_{l3\sigma} + n_{lj 3\sigma}) \\ &= - (n_{l'_i 3\sigma} + n_{l'_j 3\sigma}). \end{aligned} \quad (91)$$

Calculating $\langle \hat{P}_{i;l_i} \hat{n}_{ia\sigma} \hat{n}_{ib\sigma'} \hat{P}_{i;l_i} \rangle_0$ and $\frac{P(L-1; \{N'_{a\sigma}\})}{P(L; \{N_{a\sigma}\})}$ in Eq. (84) and $\langle \hat{P}_{i;l_i} \hat{P}_{j;l_j} \hat{c}_{ia\sigma}^\dagger \hat{c}_{jb\sigma} \hat{P}_{i;l'_i} \hat{P}_{j;l'_j} \rangle_0$ and $\frac{P(L-2; \{N''_{a\sigma}\})}{P(L; \{N_{a\sigma}\})}$ in Eq. (85) explicitly for each possible configurations, we find

$$\frac{\langle \Psi_G | \hat{n}_{ia\sigma} \hat{n}_{ib\sigma'} | \Psi_G \rangle}{\langle \Psi_G | \Psi_G \rangle} \xrightarrow{\text{GA}} \frac{1}{L} \sum'_{l_i} g_{l_i}^2 \left(\prod_l g_l^{2\Delta\bar{\Gamma}'_l} \right) \frac{\left(\prod_l \bar{\Gamma}'_l! \right)}{\left(\prod_l \bar{\Gamma}'_l! \right)}, \quad (92)$$

and

$$\frac{\langle \Psi_G | \hat{c}_{ia\sigma}^\dagger \hat{c}_{jb\sigma} | \Psi_G \rangle}{\langle \Psi_G | \Psi_G \rangle} \xrightarrow{\text{GA}} \frac{1}{L^2} \sum''_{l_i, l_j, l'_i, l'_j} g_{l_i} g_{l_j} g_{l'_i} g_{l'_j} \langle \hat{c}_{ia\sigma}^\dagger \hat{c}_{jb\sigma} \rangle_0 \left(\prod_l g_l^{2\Delta\bar{\Gamma}_l''} \right) \frac{(\prod_l \bar{\Gamma}_l!)}{(\prod_l \bar{\Gamma}_l'!)^2} \frac{1}{(1-n_a^0)n_b^0}. \quad (93)$$

In addition, we have the following relation in the thermodynamic limit:

$$\frac{(\bar{\Gamma}_l!)}{(\bar{\Gamma}_l + \Delta\bar{\Gamma}_l!)} \sim (\bar{\Gamma}_l)^{-\Delta\bar{\Gamma}_l}. \quad (94)$$

Using this relation, we can rewrite Eqs. (92) and (93) as

$$\frac{\langle \Psi_G | \hat{n}_{ia\sigma} \hat{n}_{ib\sigma'} | \Psi_G \rangle}{\langle \Psi_G | \Psi_G \rangle} \xrightarrow{\text{GA}} \frac{1}{L} \sum'_i g_{l_i}^2 \prod_l \left(\frac{\bar{\Gamma}_l}{g_l^2} \right)^{-\Delta\bar{\Gamma}_l'}, \quad (95)$$

$$\frac{\langle \Psi_G | \hat{c}_{ia\sigma}^\dagger \hat{c}_{jb\sigma} | \Psi_G \rangle}{\langle \Psi_G | \Psi_G \rangle} \xrightarrow{\text{GA}} \frac{1}{L^2} \sum''_{l_i, l_j, l'_i, l'_j} g_{l_i} g_{l_j} g_{l'_i} g_{l'_j} \langle \hat{c}_{ia\sigma}^\dagger \hat{c}_{jb\sigma} \rangle_0 \frac{1}{(1-n_a^0)n_b^0} \prod_l \left(\frac{\bar{\Gamma}_l}{g_l^2} \right)^{-\Delta\bar{\Gamma}_l''}, \quad (96)$$

respectively. Substituting Eq. (59) into these equations and using relations $L^{-\sum_i \Delta\bar{\Gamma}_l'} = L$ and $L^{-\sum_i \Delta\bar{\Gamma}_l''} = L^2$ from Eqs. (86) and (89), we find

$$\begin{aligned} \frac{\langle \Psi_G | \hat{n}_{ia\sigma} \hat{n}_{ib\sigma'} | \Psi_G \rangle}{\langle \Psi_G | \Psi_G \rangle} &\xrightarrow{\text{GA}} \sum'_i g_{l_i}^2 \exp \left[- \sum_l (1 + \lambda_0) \Delta\bar{\Gamma}_l' - \sum_{l, a', \sigma''} \lambda_{a'\sigma''} n_{la'\sigma''} \Delta\bar{\Gamma}_l' \right] \\ &= \sum'_i g_{l_i}^2 \exp \left[(1 + \lambda_0) + \sum_{a', \sigma''} \lambda_{a'\sigma''} n_{la'\sigma''} \right] \\ &= \sum'_i \frac{\bar{\Gamma}_{l_i}}{L}, \end{aligned} \quad (97)$$

$$\begin{aligned} \frac{\langle \Psi_G | \hat{c}_{ia\sigma}^\dagger \hat{c}_{jb\sigma} | \Psi_G \rangle}{\langle \Psi_G | \Psi_G \rangle} &\xrightarrow{\text{GA}} \sum''_{l_i, l_j, l'_i, l'_j} g_{l_i} g_{l_j} g_{l'_i} g_{l'_j} \langle \hat{c}_{ia\sigma}^\dagger \hat{c}_{jb\sigma} \rangle_0 \frac{1}{(1-n_a^0)n_b^0} \exp \left[- \sum_l (1 + \lambda_0) \Delta\bar{\Gamma}_l'' \right] \exp \left[- \sum_{l, a', \sigma''} \lambda_{a'\sigma''} n_{la'\sigma''} \Delta\bar{\Gamma}_l'' \right] \\ &= \sum''_{l_i, l_j, l'_i, l'_j} g_{l_i} g_{l_j} g_{l'_i} g_{l'_j} \langle \hat{c}_{ia\sigma}^\dagger \hat{c}_{jb\sigma} \rangle_0 \frac{1}{(1-n_a^0)n_b^0} \exp \left[2(1 + \lambda_0) \right] \\ &\quad \times \exp \left[\frac{1}{2} \sum_{a', \sigma'} \lambda_{a'\sigma'} (n_{la'\sigma'} + n_{lj a'\sigma'} + n_{l'_i a'\sigma'} + n_{l'_j a'\sigma'}) \right] \\ &= \frac{1}{(1-n_a^0)n_b^0} \langle \hat{c}_{ia\sigma}^\dagger \hat{c}_{jb\sigma} \rangle_0 \sum''_{l_i, l_j, l'_i, l'_j} \frac{\sqrt{\bar{\Gamma}_{l_i} \bar{\Gamma}_{l_j} \bar{\Gamma}_{l'_i} \bar{\Gamma}_{l'_j}}}{L^2}. \end{aligned} \quad (98)$$

In deriving Eq. (98), we have also used the following relation due to Eq. (63):

$$\sum_{a=1,2} \lambda_{a\sigma} (n_{l'_i a\sigma} + n_{l'_j a\sigma}) = \sum_{a=1,2} \lambda_{a\sigma} (n_{l_i a\sigma} + n_{l_j a\sigma}). \quad (99)$$

Finally, the variational energy becomes

$$\begin{aligned} E_{\text{gs}} &\xrightarrow{\text{GA}} \min_{\{g_l\}} \left[- \sum_{i,j} \sum_{a,b=1}^2 \sum_{\sigma=\uparrow,\downarrow} t_{ab}^{i,j}(\phi) \frac{1}{(1-n_1^0)n_1^0} \langle \hat{c}_{ia\sigma}^\dagger \hat{c}_{jb\sigma} \rangle_0 \sum''_{l_i, l_j, l'_i, l'_j} \frac{\sqrt{\bar{\Gamma}_{l_i} \bar{\Gamma}_{l_j} \bar{\Gamma}_{l'_i} \bar{\Gamma}_{l'_j}}}{L^2} \right. \\ &\quad - \sum_{i,j} \sum_{a,b=3} \sum_{\sigma=\uparrow,\downarrow} t_{ab}^{i,j}(\phi) \frac{1}{(1-n_3^0)n_3^0} \langle \hat{c}_{ia\sigma}^\dagger \hat{c}_{jb\sigma} \rangle_0 \sum''_{l_i, l_j, l'_i, l'_j} \frac{\sqrt{\bar{\Gamma}_{l_i} \bar{\Gamma}_{l_j} \bar{\Gamma}_{l'_i} \bar{\Gamma}_{l'_j}}}{L^2} \\ &\quad \left. + U \sum_i \sum_{a=b} \sum_{\sigma=\uparrow} \sum_{\sigma'=\downarrow} \sum_{l_i} \frac{\bar{\Gamma}_{l_i}}{L} + U' \sum_i \sum_{a>b} \sum_{\sigma, \sigma'} \sum_{l_i} \frac{\bar{\Gamma}_{l_i}}{L} - J_{\text{H}} \sum_i \sum_{a>b} \sum_{\sigma=\sigma'} \sum_{l_i} \frac{\bar{\Gamma}_{l_i}}{L} \right]. \end{aligned} \quad (100)$$

TABLE I: The configurations, the wave functions, the values of \hat{H}_{int} , and the variational parameters g_{X_k} for a PM state consisting of the degenerate d_{xz} and d_{yz} orbitals and the d_{xy} orbital. 0 and \uparrow (\downarrow) in the wave functions mean there are no electrons in orbital a with spin σ and there is a spin-up (spin-down) electron in orbital a , respectively.

	Wave functions	value of \hat{H}_{int}	g_{X_k}
X_0	$ 0, 0; 0, 0; 0, 0\rangle$	0	g_{X_0}
X_1	$ \uparrow, 0; 0, 0; 0, 0\rangle, 0, \downarrow; 0, 0; 0, 0\rangle, 0, 0; \uparrow, 0; 0, 0\rangle, 0, 0; 0, \downarrow; 0, 0\rangle$	0	g_{X_1}
X_2	$ 0, 0; 0, 0; \uparrow, 0\rangle, 0, 0; 0, 0; \downarrow\rangle$	0	g_{X_2}
X_3	$ \uparrow, \downarrow; 0, 0; 0, 0\rangle, 0, 0; \uparrow, \downarrow; 0, 0\rangle$	U	g_{X_3}
X_4	$ 0, 0; 0, 0; \uparrow, \downarrow\rangle$	U	g_{X_4}
X_5	$ \uparrow, 0; 0, \downarrow; 0, 0\rangle, 0, \downarrow; \uparrow, 0; 0, 0\rangle,$	U'	g_{X_5}
X_6	$ \uparrow, 0; 0, 0; 0, \downarrow\rangle, 0, \downarrow; 0, 0; \uparrow, 0\rangle, 0, 0; \uparrow, 0; 0, \downarrow\rangle, 0, 0; 0, \downarrow; \uparrow, 0\rangle$	U'	g_{X_6}
X_7	$ \uparrow, 0; \uparrow, 0; 0, 0\rangle, 0, \downarrow; 0, \downarrow; 0, 0\rangle$	$U' - J_{\text{H}}$	g_{X_7}
X_8	$ \uparrow, 0; 0, 0; \uparrow, 0\rangle, 0, \downarrow; 0, 0; 0, \downarrow\rangle, 0, 0; \uparrow, 0; \uparrow, 0\rangle, 0, 0; 0, \downarrow; 0, \downarrow\rangle$	$U' - J_{\text{H}}$	g_{X_8}
X_9	$ \uparrow, \downarrow; \uparrow, 0; 0, 0\rangle, \uparrow, \downarrow; 0, \downarrow; 0, 0\rangle, \uparrow, 0; \uparrow, \downarrow; 0, 0\rangle, 0, \downarrow; \uparrow, \downarrow; 0, 0\rangle$	$U + 2U' - J_{\text{H}}$	g_{X_9}
X_{10}	$ \uparrow, \downarrow; 0, 0; \uparrow, 0\rangle, \uparrow, \downarrow; 0, 0; 0, \downarrow\rangle, 0, 0; \uparrow, \downarrow; \uparrow, 0\rangle, 0, 0; \uparrow, \downarrow; 0, \downarrow\rangle$	$U + 2U' - J_{\text{H}}$	$g_{X_{10}}$
X_{11}	$ \uparrow, 0; 0, 0; \uparrow, \downarrow\rangle, 0, \downarrow; 0, 0; \uparrow, \downarrow\rangle, 0, 0; \uparrow, 0; \uparrow, \downarrow\rangle, 0, 0; 0, \downarrow; \uparrow, \downarrow\rangle$	$U + 2U' - J_{\text{H}}$	$g_{X_{11}}$
X_{12}	$ \uparrow, 0; 0, \downarrow; 0, \downarrow\rangle, 0, \downarrow; \uparrow, 0; \uparrow, 0\rangle, \uparrow, 0; 0, \downarrow; \uparrow, 0\rangle, 0, \downarrow; \uparrow, 0; 0, \downarrow\rangle, \uparrow, 0; \uparrow, 0; 0, \downarrow\rangle, 0, \downarrow; 0, \downarrow; \uparrow, 0\rangle$	$3U' - J_{\text{H}}$	$g_{X_{12}}$
X_{13}	$ \uparrow, 0; \uparrow, 0; \uparrow, 0\rangle, 0, \downarrow; 0, \downarrow; 0, \downarrow\rangle$	$3U' - 3J_{\text{H}}$	$g_{X_{13}}$
X_{14}	$ \uparrow, \downarrow; \uparrow, 0; 0, \downarrow\rangle, \uparrow, \downarrow; 0, \downarrow; \uparrow, 0\rangle, \uparrow, 0; \uparrow, \downarrow; 0, \downarrow\rangle, 0, \downarrow; \uparrow, \downarrow; \uparrow, 0\rangle$	$U + 5U' - 2J_{\text{H}}$	$g_{X_{14}}$
X_{15}	$ \uparrow, 0; 0, \downarrow; \uparrow, \downarrow\rangle, 0, \downarrow; \uparrow, 0; \uparrow, \downarrow\rangle$	$U + 5U' - 2J_{\text{H}}$	$g_{X_{15}}$
X_{16}	$ \uparrow, \downarrow; \uparrow, 0; \uparrow, 0\rangle, \uparrow, \downarrow; 0, \downarrow; 0, \downarrow\rangle, \uparrow, 0; \uparrow, \downarrow; \uparrow, 0\rangle, 0, \downarrow; \uparrow, \downarrow; 0, \downarrow\rangle$	$U + 5U' - 3J_{\text{H}}$	$g_{X_{16}}$
X_{17}	$ \uparrow, 0; \uparrow, 0; \uparrow, \downarrow\rangle, 0, \downarrow; 0, \downarrow; \uparrow, \downarrow\rangle$	$U + 5U' - 3J_{\text{H}}$	$g_{X_{17}}$
X_{18}	$ \uparrow, \downarrow; \uparrow, \downarrow; 0, 0\rangle$	$2U + 4U' - 2J_{\text{H}}$	$g_{X_{18}}$
X_{19}	$ \uparrow, \downarrow; 0, 0; \uparrow, \downarrow\rangle, 0, 0; \uparrow, \downarrow; \uparrow, \downarrow\rangle$	$2U + 4U' - 2J_{\text{H}}$	$g_{X_{19}}$
X_{20}	$ \uparrow, 0; \uparrow, \downarrow; \uparrow, \downarrow\rangle, 0, \downarrow; \uparrow, \downarrow; \uparrow, \downarrow\rangle, \uparrow, \downarrow; \uparrow, 0; \uparrow, \downarrow\rangle, \uparrow, \downarrow; 0, \downarrow; \uparrow, \downarrow\rangle$	$2U + 8U' - 4J_{\text{H}}$	$g_{X_{20}}$
X_{21}	$ \uparrow, \downarrow; \uparrow, \downarrow; \uparrow, 0\rangle, \uparrow, \downarrow; \uparrow, \downarrow; 0, \downarrow\rangle$	$2U + 8U' - 4J_{\text{H}}$	$g_{X_{21}}$
X_{22}	$ \uparrow, \downarrow; \uparrow, \downarrow; \uparrow, \downarrow\rangle$	$3U + 12U' - 6J_{\text{H}}$	$g_{X_{22}}$

Here, the restrictions about the summations with respect to l_i , l_j , l'_i , and l'_j in the first and second terms are those for the hopping process $\hat{c}_{ia\sigma}^\dagger \hat{c}_{jb\sigma}$ ($a, b = 1, 2$) and hopping process $\hat{c}_{i3\sigma}^\dagger \hat{c}_{j3\sigma}$, and the restrictions about the summations with respect to l_i in the third, fourth, and final terms are those for the interaction terms U , U' , and J_{H} . In deriving Eq. (100), we have neglected the term of \hat{H}_{CEF} in the variational energy since this term only gives a constant energy shift which is independent on the strength of the onsite interactions within the present treatment. Note that E_{gs} can be written as the products of the component for orbital a with spin σ since we have neglected both J' and the transverse components of J_{H} in the interacting Hamiltonian as denoted in Sec. II.

For simplicity of the numerical calculation, we classify the possible 64 configurations into 23 groups in which the energies are same. These are shown in Table I, where X_k denotes the optimized number of sites with the configuration in the k group; e.g., $X_1 = \bar{\Gamma}_l$ for $l = 1 - 4$, and so on. Denoting $x_k = X_k/L$, we obtain

$$\begin{aligned}
E_{\text{gs}} \xrightarrow{\text{GA}} \min_{x_3, x_4, \dots, x_{22}} & \left[- \sum_{i,j} \sum_{a,b=1}^3 \sum_{\sigma} q_{ab}(x_3, x_4, \dots, x_{22}) t_{ab}^{i,j}(\phi) \langle \hat{c}_{ia\sigma}^\dagger \hat{c}_{jb\sigma} \rangle_0 \right. \\
& + U(2x_3 + x_4 + 4x_9 + 4x_{10} + 4x_{11} + 4x_{14} + 2x_{15} + 4x_{16} + 2x_{17} + 2x_{18} + 4x_{19} + 8x_{20} \\
& \quad \left. + 4x_{21} + 3x_{22}) \right. \\
& + U'(2x_5 + 4x_6 + 4x_9 + 4x_{10} + 4x_{11} + 12x_{12} + 12x_{14} + 6x_{15} + 8x_{16} + 4x_{17} + 2x_{18} + 4x_{19} \\
& \quad \left. + 16x_{20} + 8x_{21} + 6x_{22}) \right. \\
& + (U' - J_{\text{H}})(2x_7 + 4x_8 + 4x_9 + 4x_{10} + 4x_{11} + 6x_{12} + 6x_{13} + 8x_{14} + 4x_{15} + 12x_{16} + 6x_{17} \\
& \quad \left. + 2x_{18} + 4x_{19} + 16x_{20} + 8x_{21} + 6x_{22}) \right]. \tag{101}
\end{aligned}$$

Here, $q_{ab}(x_3, x_4, \dots, x_{22})$ is the RF of the kinetic energy for the Ru t_{2g} orbital, which satisfies

$$q_{11}(x_3, x_4, \dots, x_{22}) = q_{12}(x_3, x_4, \dots, x_{22}) = q_{21}(x_3, x_4, \dots, x_{22}) = q_{22}(x_3, x_4, \dots, x_{22}). \quad (102)$$

The RFs for the $d_{xz/yz}$ and d_{xy} orbitals are given by

$$\begin{aligned} q_{11}(x_3, x_4, \dots, x_{22}) = \frac{1}{n_1^0(1 - n_1^0)} & \left[\sqrt{x_1}(\sqrt{x_0} + \sqrt{x_3} + \sqrt{x_5} + \sqrt{x_7}) + \sqrt{x_6}(\sqrt{x_2} + \sqrt{x_{10}} + 2\sqrt{x_{12}}) \right. \\ & + \sqrt{x_8}(\sqrt{x_2} + \sqrt{x_{10}} + \sqrt{x_{12}} + \sqrt{x_{13}}) + \sqrt{x_9}(\sqrt{x_3} + \sqrt{x_5} + \sqrt{x_7} + \sqrt{x_{18}}) \\ & + \sqrt{x_{11}}(\sqrt{x_4} + \sqrt{x_{15}} + \sqrt{x_{17}} + \sqrt{x_{19}}) + \sqrt{x_{14}}(\sqrt{x_{10}} + 2\sqrt{x_{12}} + \sqrt{x_{21}}) \\ & \left. + \sqrt{x_{16}}(\sqrt{x_{10}} + \sqrt{x_{12}} + \sqrt{x_{13}} + \sqrt{x_{21}}) + \sqrt{x_{20}}(\sqrt{x_{15}} + \sqrt{x_{17}} + \sqrt{x_{19}} + \sqrt{x_{22}}) \right]^2, \end{aligned} \quad (103)$$

and

$$\begin{aligned} q_{33}(x_3, x_4, \dots, x_{22}) = \frac{1}{n_3^0(1 - n_3^0)} & \left[\sqrt{x_2}(\sqrt{x_0} + \sqrt{x_4}) + 2\sqrt{x_1}(\sqrt{x_6} + \sqrt{x_8}) + 2\sqrt{x_{10}}(\sqrt{x_3} + \sqrt{x_{19}}) \right. \\ & + 2\sqrt{x_{11}}(\sqrt{x_6} + \sqrt{x_8}) + 2\sqrt{x_{12}}(\sqrt{x_5} + \sqrt{x_{15}}) + \sqrt{x_{17}}(\sqrt{x_{12}} + \sqrt{x_{13}}) \\ & + \sqrt{x_7}(\sqrt{x_{12}} + \sqrt{x_{13}}) + 2\sqrt{x_9}(\sqrt{x_{14}} + \sqrt{x_{16}}) + 2\sqrt{x_{20}}(\sqrt{x_{14}} + \sqrt{x_{16}}) \\ & \left. + \sqrt{x_{21}}(\sqrt{x_{18}} + \sqrt{x_{22}}) \right]^2, \end{aligned} \quad (104)$$

respectively. Note that the optimization with respect to $\{g_{X_k}\}$ is equivalent that with respect to $\{x_k\}$ due to the relation $x_k = g_{X_k}^2 \exp(1 + \lambda_0 + \sum_{a,\sigma} \lambda_{a\sigma} n_{la\sigma})$. In the numerical calculations, we use the following constraints instead of determining the Lagrange multipliers λ_0 and $\lambda_{a\sigma}$:

$$1 = x_0 + 4x_1 + 2x_2 + 2x_3 + x_4 + 2x_5 + 4x_6 + 2x_7 + 4x_8 + 4x_9 + 4x_{10} + 4x_{11} + 6x_{12} + 2x_{13} + 4x_{14} + 2x_{15} + 4x_{16} + 2x_{17} + x_{18} + 2x_{19} + 4x_{20} + 2x_{21} + x_{22}, \quad (105)$$

$$n_1^0 = x_1 + x_3 + x_5 + x_6 + x_7 + x_8 + 3x_9 + 2x_{10} + x_{11} + 3x_{12} + x_{13} + 3x_{14} + x_{15} + 3x_{16} + x_{17} + x_{18} + x_{19} + 3x_{20} + 2x_{21} + x_{22}, \quad (106)$$

$$n_3^0 = x_2 + x_4 + 2x_6 + 2x_8 + 2x_{10} + 4x_{11} + 3x_{12} + x_{13} + 2x_{14} + 2x_{15} + 2x_{16} + 2x_{17} + 2x_{19} + 4x_{20} + x_{21} + x_{22}. \quad (107)$$

III. RESULTS

In this section, we show the numerical results of the GA for three cases with the effective models of $x = 2$ and 0.5 and the special model. The variational energy Eq. (101) is numerically minimized with respect to $\{x_k\}$ under the constraints (105)–(107) by Powell's method,³⁴ which is one of the numerical methods to minimize a function with more than one variable. In this work, we use the value of U as the parameter, and set $U' = U - 2J_H$, $J_H = U/4$, and $W_{\text{tot}} = 4.1$ eV, which is obtained in the effective model of $x = 2$.

A. Mass enhancement for the effective models of $x = 2$ and 0.5

We first show the results for the effective models of $x = 2$ and 0.5. Figures 9 and 10 represent the RFs of the kinetic energy for the Ru t_{2g} orbitals as a function of U/W_{tot} for these models. We see from Fig. 9 that the RFs for the $d_{xz/yz}$ and d_{xy} orbitals are nearly the same

for the case of $x = 2$. This is probably originated from the fact that these orbitals have nearly the same occupation numbers (i.e., $n_1^0 = n_2^0 = n_3^0 = 4/3$) in the absence of the interactions. On the other hands, for the case of $x = 0.5$, we find from Fig. 10 that the RFs for the $d_{xz/yz}$ and d_{xy} orbitals are different, and that the increase of U/W_{tot} leads to the large difference between these RFs. The occupation number for each Ru t_{2g} orbital becomes $(n_1^0, n_2^0, n_3^0) = (1.17, 1.17, 1.66)$ for the case of $x = 0.5$. This change of the occupation numbers results mainly from the downward shift of the d_{xy} orbital since we have $(n_1^0, n_2^0, n_3^0) = (1.32, 1.32, 1.35)$, which are little different from those for the case of $x = 2$, for the model setting $\phi = 15^\circ$ and $\Delta_{t_{2g}} = 0$ eV in Eq. (48). By using the analogy with the result for the single-orbital Hubbard model, the difference of the RFs between the cases of $x = 2$ and $x = 0.5$ will be due to this change of the occupation numbers approaching the integer values towards $x = 0.5$, which is expected in the usual Mott transition; in the present case, the occupation numbers expected in the Mott insulator are 1 for the $d_{xz/yz}$ orbital and 2 for the d_{xy} orbital, respectively.

In order to compare our results with the experimen-

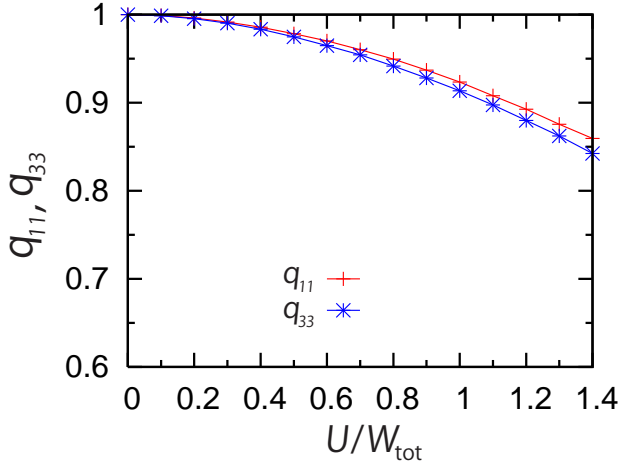


FIG. 9: (Color online) RFs for the $d_{xz/yz}$ and d_{xy} orbitals as a function of U/W_{tot} for the effective model of $x = 2$. We set $J_{\text{H}} = U/4$.

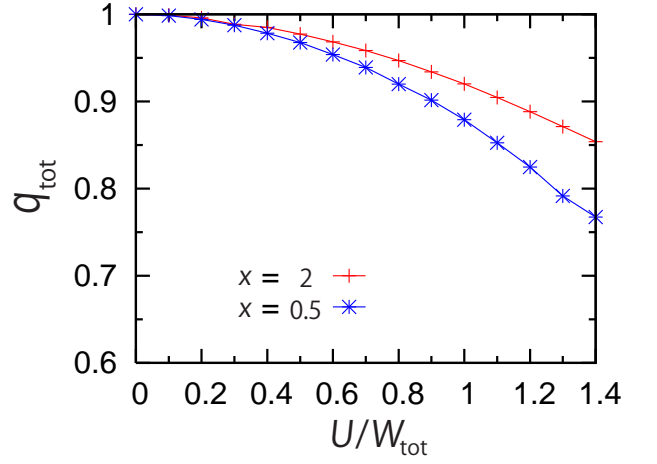


FIG. 11: (Color online) Total RFs as a function of U/W_{tot} for the effective models of $x = 2$ and 0.5 . We set $J_{\text{H}} = U/4$.

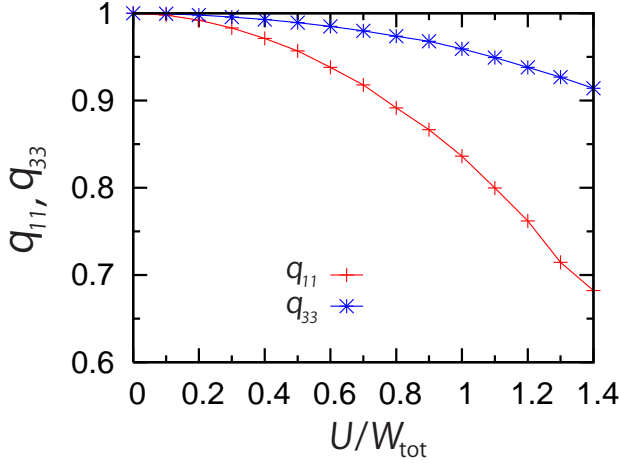


FIG. 10: (Color online) RFs for the $d_{xz/yz}$ and d_{xy} orbitals as a function of U/W_{tot} for the effective model of $x = 0.5$. We set $J_{\text{H}} = U/4$.

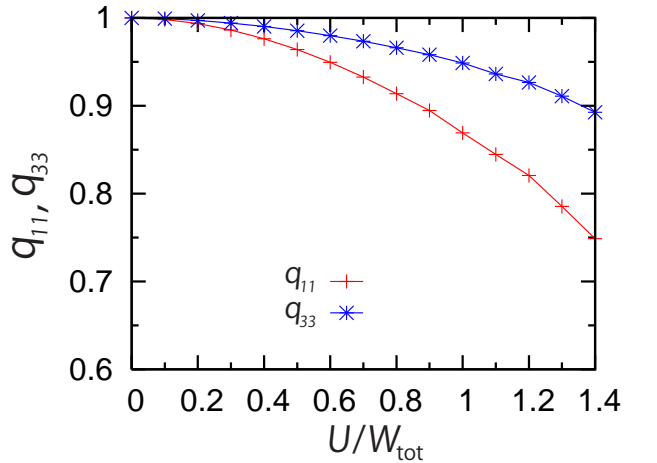


FIG. 12: (Color online) RFs for the $d_{xz/yz}$ and d_{xy} orbitals as a function of U/W_{tot} for the special model. We set $J_{\text{H}} = U/4$.

tally observed mass enhancement, we define a total RF,

$$q_{\text{tot}} = \sqrt{\frac{1}{3} \sum_{a=1}^3 q_{aa}^2}, \quad (108)$$

which estimates the inverse of the mass enhancement. Figure 11 shows the total RFs as a function of U/W_{tot} for the effective models of $x = 2$ and 0.5 . We see that q_{tot} for the case of $x = 0.5$ becomes much smaller than that for the case of $x = 2$ as U/W_{tot} increases. Therefore, our results suggest that moderately strong Coulomb interaction and the modifications of the electronic structures for the Ru t_{2g} orbitals due to the rotation of RuO₆ octahedra lead to mass enhancement for $x = 0.5$ than that for $x = 2$.

B. Primary effect of the Ca substitution

on mass enhancement around $x = 0.5$

In order to clarify the role of the Ca substitution in forming the HF, we calculate the RF for the special model. Figure 12 shows the RFs for each Ru t_{2g} orbital. We see that the RF for the $d_{xz/yz}$ orbital is slightly larger than that for the case of $x = 0.5$, while the RF for the d_{xy} orbital is slightly smaller. The former results mainly from the decrease of the occupation number for the $d_{xz/yz}$ orbital from 1.21 to 1.17, and the latter results mainly from the increase of the occupation number for the d_{xy} orbital from 1.57 to 1.66; both changes of the occupation numbers arise from the downward shift for the d_{xy} orbital, which is induced by the rotation of RuO₆ octahedra.

Figure 13 shows the total RFs for both the effective model of $x = 0.5$ and the special model. We find that the inverse of q_{tot} for the effective model of $x = 0.5$ is larger than that for the special model, and that Coulomb

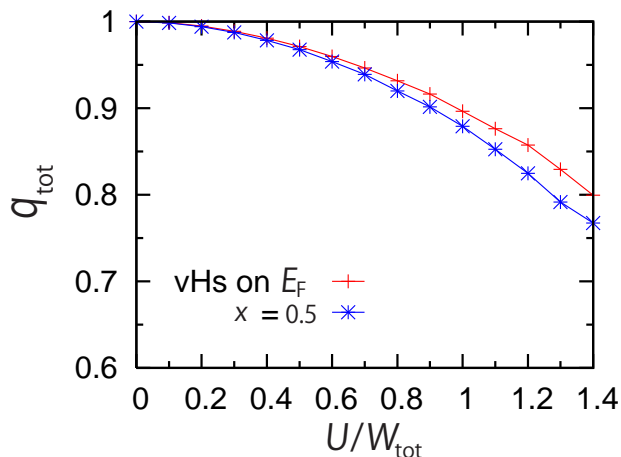


FIG. 13: (Color online) Total RFs as a function of U/W_{tot} for the effective model of $x = 0.5$ and the special model. We set $J_H = U/4$.

interaction enhances this difference of the inverse of q_{tot} . Therefore, our result indicates that the vHs for the d_{xy} orbital plays a secondary role in enhancing the effective mass around $x = 0.5$; the primary one arises from the change of the occupation numbers approaching the integer values. Note that these occupation numbers are different from those expected in the OSMT but same to those expected in the usual Mott transition, where the occupation numbers for the $d_{xz/yz}$ and d_{xy} orbitals are 1 and 2, respectively.

IV. DISCUSSION

A. Comparison with previous theoretical studies

We first remark on the physical meaning of the enhancement of the effective mass obtained in the GA. For simplicity, we consider a PM state consisting of a single orbital. The following argument is based on the discussion in Ref. 33. One of the origins of the HF behavior is the criticality approaching the Mott transition. Namely, the formation of the HF results from separation of energy scale between spin and charge degrees of freedom due to electron correlation; on-site charge fluctuation suppresses at the higher scale corresponding to U , and the lower one, T_F^* , associates with the local spin fluctuation. Below T_F^* , a Fermi-liquid description applies; the mass enhancement is inversely proportional to a ratio of T_F^* to the noninteracting Fermi temperature. Although the analysis using the GA restricts to the discussion about the properties for the ground states and can not address the possibility of the above separation of energy scale, the GA can analyze the effective mass for systems with a different parameter. A similar argument can apply to a system with orbital degrees of freedom. Therefore, we think that the analysis using the GA can capture the tendency of mass enhancement in $\text{Ca}_{2-x}\text{Sr}_x\text{RuO}_4$ for $0.5 \leq x \leq 2$.

In the present calculation, we have not discussed Mott transition. From a theoretical point of view, the previous DMFT calculation¹⁹ based on the models for $\text{Ca}_{2-x}\text{Sr}_x\text{RuO}_4$ in $0.5 \leq x \leq 2$ has shown that the critical value of U for the Mott transition, U_c , at $x = 0.5$ is larger than 6 eV (i.e., $U/W_{\text{tot}} > 1.4$) at $T = 0.02$ eV. In principle, the Gutzwiller-type variational wave function gives the Mott transition as a function of U , when charge fluctuations, which play an important role in the vicinity of the Mott transition,³⁶ are included.³⁷⁻⁴¹ However, the present study using the GA is inappropriate to address the possibility of the Mott transition. Thus, we have shown the results only for the case with $U/W_{\text{tot}} \leq 1.4$ where the system will remain metallic.

The present formalism of the GA neglects the variation of the occupation number for each orbital due to electron correlation for simplicity. The previous DMFT calculation¹⁹ based on the models for $\text{Ca}_{2-x}\text{Sr}_x\text{RuO}_4$ with $0.5 \leq x \leq 2$ has observed a drastic variation of the occupation numbers ($\sim 20 - 30\%$) for values of U near U_c , while the variation is about 10% (a few %) for $U \sim 0.8U_c$ ($U \sim 0.7U_c$). This indicates that the variation of the occupation numbers due to electron correlation is important near the Mott transition. In this paper, we have discussed the HF behavior only in the regions where the effects of the variation of the occupation numbers is small.

Although it will be necessary to include the variation of the occupation number for each orbital for the quantitative argument, we think from the following arguments that the obtained tendency of the mass enhancement in $0.5 \leq x \leq 2$ does not change qualitatively even if the variation of the occupation number for each orbital is included. According to the DMFT study¹⁹ for the three-orbital Hubbard model, U_c decreases when the occupation number for each orbital in the absence of interactions approaches to an integer value. Simultaneously, the occupation number for each orbital changes as a function of U/W_{tot} . Since the decrease of U_c leads to the increase of the effective mass at a fixed value of U/W_{tot} and J_H/U , the mass enhancement will be largest at $x = 0.5$ where the occupation numbers in the absence of interactions are nearest to integer values in $0.5 \leq x \leq 2$. Therefore, our results about the mass enhancement in $0.5 \leq x \leq 2$ will not change qualitatively even if the variation of the occupation number for each orbital is included.

DMFT studies⁴²⁻⁴⁴ proposed that the Hund's rule coupling plays an important role in stabilizing a metallic state with large effective mass. For example, a DMFT study⁴⁴ for the degenerate three-orbital Hubbard model showed that the increase of J_H/U leads to a decrease of U_c at $\frac{1}{2}$ -filling and an increase of U_c at $\frac{1}{6}$ -filling. (Note that there are three electrons per a site at $\frac{1}{2}$ -filling and there is one electron per a site at $\frac{1}{6}$ -filling.) From this result, they claimed that the increase of J_H/U extends a region for the metallic state with large effective mass at the filling away from $\frac{1}{2}$ -filling; this metallic state is called Hund's metal. However, in $\text{Ca}_{2-x}\text{Sr}_x\text{RuO}_4$, the

total filling number does not change in $0.5 \leq x \leq 2$ (i.e., $\frac{2}{3}$ -filling) and the value of J_H/U does not change either. The main changes due to the Ca substitution are both the bandwidth for each Ru t_{2g} orbital and the occupation number for each Ru t_{2g} orbital. Therefore, the effect of the Hund's rule coupling is not important for the difference between $x = 0.5$ and 2. Instead, the criticality approaching the Mott transition plays a more important role in enhancing the effective mass in $\text{Ca}_{2-x}\text{Sr}_x\text{RuO}_4$ towards $x = 0.5$.

We now address the effect of the neglected terms in the interacting Hamiltonian (i.e., J' and the transverse components of J_H) on the electronic states. According to the previous study²⁵ of the PM state for the two-orbital Hubbard model in the GA, these terms slightly stabilize a PM metal against a nonmagnetic insulator. This result suggests that the effect of these neglected terms little affects the properties for the PM state studied in the present study within the GA. On the other hand, the transverse components of J_H will strongly affect the stability of the magnetically ordered states. Therefore, these neglected terms will not change the obtained tendency of the mass enhancement in PM states.

According to the density-functional calculation for $\text{Ca}_{2-x}\text{Sr}_x\text{RuO}_4$ in $0.5 \leq x \leq 2$ within the LDA,³³ the total bandwidth for the Ru t_{2g} orbitals becomes smaller for $x = 0.5$ than that for $x = 2$. Although this reduction is partially included in our calculation through the ϕ dependence of the dispersions, it seems that these are other effects which reduce the total band width. Thus, if this effect is fully included, the difference between the values of q_{tot}^{-1} for $x = 2$ and 0.5 will become larger than for the present calculation.

In our analysis, we have assumed that the roles of the O $2p$ orbitals are only to change the dp hybridizations. However, the previous theoretical work⁴⁵ based on the dp model for Sr_2RuO_4 has proposed that Coulomb interaction for the O $2p$ orbitals plays an important role in stabilizing spin-triplet superconductivity. We expect that the Coulomb interaction for the O $2p$ orbitals leads to a larger mass enhancement than the present calculation. The more detailed theoretical study about the role of the O $2p$ orbitals is deserved.

There is a theoretical proposal that the vHs for the d_{xy} orbital plays a primary role in forming HF's around $x = 0.5$ on the basis of the density-functional calculation within the LDA.⁴⁶ This work has proposed that the rotation-induced hybridization of the d_{xy} orbital to the $d_{x^2-y^2}$ orbital causes the magnetic instability due to the nesting of the FS for the d_{xy} orbital, and that the instability will lead to the mass enhancement around $x = 0.5$. In contrast, our results suggest that the primary role arises from the criticality approaching the usual Mott transition resulting from the change of the occupation numbers for the Ru t_{2g} orbitals due to the downward shift of the d_{xy} orbital, and not from the vHs. It will be necessary to study the effect of the vHs on the formation of HF's around $x = 0.5$ more systematically.

B. Correspondence with experimental results

We first discuss the roles of the Ru e_g and O $2p$ orbitals in determining the electronic states for $\text{Ca}_{2-x}\text{Sr}_x\text{RuO}_4$ in $0.5 \leq x \leq 2$. In this study, we have taken account of the effects of these orbitals as the changes of the dp hybridization and the CEF energy for the Ru t_{2g} orbitals; the latter is the downward shift of the d_{xy} orbital due to the hybridization with the $d_{x^2-y^2}$ orbital. There is no experimental evidence that the Ru e_g orbitals play an important role in determining the electronic states except the possible change of the CEF energy through the hybridization of the Ru t_{2g} orbitals; thus, our treatment about the Ru e_g orbitals will be valid. In contrast, a polarized neutron diffraction measurement for $\text{Ca}_{1.5}\text{Sr}_{0.5}\text{RuO}_4$ has observed a field-induced magnetic moment on the in-plane O ions, which is about 20% of that for Ru ions.⁴⁷ This result indicates that not only the dp hybridizations, but also the Coulomb interaction for the O $2p$ orbitals will play non-negligible roles in determining the electronic states. It is thus necessary to study the role of the O $2p$ orbitals systematically.

Let us remark on the role of the spin-orbit interaction, which has been neglected in this work. The experimentally observed FSS^{20,32} for $x = 2$ and 0.5 are reproducible by the density-function calculations without the spin-orbit interaction.^{27,28,33} Therefore, the spin-orbit interaction will be negligible in determining the electronic states.

We have also neglected the effect of the disorder induced by the Ca substitution in this work. A measurement with a SQUID magnetometer for $\text{Ca}_{1.5}\text{Sr}_{0.5}\text{RuO}_4$ has observed glassy behavior (i.e., the time-dependent magnetization),¹³ which is similar to the behavior observed in $\text{Ca}_{0.95}\text{Sr}_{0.05}\text{RuO}_3$.⁴⁸ This behavior is related to the disorder by the Ca substitution. It is thus necessary to include the effect of the disorder on the electronic state in order to discuss the electronic states for $\text{Ca}_{2-x}\text{Sr}_x\text{RuO}_4$. This remains as a future problem.

Let us discuss the role of the vHs for the d_{xy} orbital. Experimentally, substitution of La^{3+} for Sr^{2+} in Sr_2RuO_4 leads to the downward shift of the vHs towards the Fermi level without any structural distortions.⁴⁹ In this case, the coefficient of the electronic specific heat for $\text{Sr}_{1.8}\text{La}_{0.2}\text{RuO}_4$ reaches 1.3 times of that in Sr_2RuO_4 .⁵⁰ This mass enhancement is mainly due to the increase of the DOS by the vHs for the d_{xy} orbital; the density-functional calculation within the LDA and the ARPES measurement support this mechanism.^{49,51} However, in the case of $\text{Ca}_{2-x}\text{Sr}_x\text{RuO}_4$ with $x = 0.5$, the ARPES measurement²⁰ has shown that the vHs is located below the Fermi level. Therefore, there must be other factors other than the vHs in enhancing the effective mass in $\text{Ca}_{2-x}\text{Sr}_x\text{RuO}_4$; our results indicate that one of the factors is the criticality approaching the usual Mott transition.

We next remark on the roles of the spin fluctuations. Around $x = 0.5$, the resistivity behaves metallic (i.e.,

$d\rho/dT > 0$), and the spin susceptibility shows Curie-Weiss behavior, as described in Sec. I. These experimental facts indicate that the mode-mode coupling for the spin fluctuations plays an important role in the electronic states around $x = 0.5$ since the enhancement of the mode-mode coupling generally leads to the Curie-Weiss behavior.⁵² The study taking account of the mode-mode coupling is a remaining future problem.

There are several experimental results which indicate that ferromagnetic spin fluctuation also plays an important role in the electronic states around $x = 0.5$. One of the examples is the enhancement of the Wilson ratio towards $x = 0.5$.⁷ This result indicates that the system is a nearly ferromagnetic metal near $x = 0.5$.^{53,54} In addition, the inelastic neutron scattering measurement⁵⁵ has claimed that the value of γ_e for $x = 0.62$ is reproducible by a phenomenological theory,⁵⁶ including the over-damped magnetic excitations for the ferromagnetic fluctuation. However, the additional Ca substitution does not lead to ferromagnetism but evolves the short-range antiferromagnetic correlation in $0.2 \leq x < 0.5$ and the long-range antiferromagnetic correlation in $0 \leq x < 0.2$.⁷ This experimental fact suggests that $\text{Ca}_{2-x}\text{Sr}_x\text{RuO}_4$ around $x = 0.5$ can not be regarded as a simple nearly ferromagnetic metal. Furthermore, the value of γ_e for $x = 2$ is insensitive to the magnetic fields up to 14 T, indicating that the mass enhancement for $x = 2$ is not due to spin fluctuations.⁵⁷ It is thus needed to study the role of the ferromagnetic spin fluctuation.

V. SUMMARY

In order to clarify the origin of the HF behavior around $x = 0.5$, we have studied the electronic states for $\text{Ca}_{2-x}\text{Sr}_x\text{RuO}_4$ in $0.5 \leq x \leq 2$ within the GA on the basis of the three-orbital Hubbard model for the Ru t_{2g} orbitals. We have assumed that the Ca substitution af-

fects the electronic structures mainly by the changes of the dp hybridizations between the Ru $4d$ and O $2p$ orbitals, and have estimated the mass enhancement on the basis of the models taking account of these effects on the electronic structures. In particular, we have numerically calculated the RF within the GA for three cases with the effective models of $x = 2$ and 0.5 and the special model. We have found that the inverse of the total RF becomes the largest for the case of $x = 0.5$, and that the vHs for the d_{xy} orbital plays a secondary role in enhancing the effective mass. Our results can reproduce the experimentally observed tendency of the effective mass in $0.5 \leq x \leq 2$:¹³ the coefficient of the electronic specific heat monotonically increases towards $x = 0.5$ although the vHs appears on the Fermi level at smaller Sr concentration than $x = 0.5$.

Our calculation suggests that the HF behavior around $x = 0.5$ comes from the cooperative effects between moderately strong Coulomb interaction compared to the total bandwidth and the modification of the electronic structures due to the rotation of RuO_6 octahedra (i.e., the variation of the $dp\pi$ hybridizations and the downward shift for the d_{xy} orbital). We propose that moderately strong electron correlation and the orbital-dependent modifications of the electronic structures due to the lattice distortions play important roles in the electronic states for $\text{Ca}_{2-x}\text{Sr}_x\text{RuO}_4$.

Acknowledgments

The authors would like to thank Y. Yanase, H. Watanabe, and T. Kariyado for useful comments. This work is supported by a Grant-in-Aid for Scientific Research on Innovative Areas ‘‘Heavy Electrons’’ (No. 20102008) of The Ministry of Education, Culture, Sports, Science, and Technology, Japan.

* Electronic address: arakawa@hosi.phys.s.u-tokyo.ac.jp

¹ C.-H. Lee, A. Iyo, H. Eisaki, H. Kito, M. T. F. Diaz, T. Ito, K. Kihou, H. Matsuhata, M. Braden, and K. Yamada, *J. Phys. Soc. Jpn.* **77**, 083704 (2008).

² R. von Helmolt, J. Wecker, B. Holzapfel, L. Schultz, and K. Samwer, *Phys. Rev. Lett.* **71**, 2331 (1993).

³ Y. Tokura, A. Urushibara, Y. Moritomo, T. Arima, A. Asamitsu, G. Kido, and N. Furukawa, *J. Phys. Soc. Jpn.* **63**, 3931 (1994).

⁴ Y. Murakami, H. Kawada, H. Kawata, M. Tanaka, T. Arima, Y. Moritomo, and Y. Tokura, *Phys. Rev. Lett.* **80**, 1932 (1998).

⁵ E. Saitoh, S. Okamoto, K. T. Takahashi, K. Tobe, K. Yamamoto, T. Kimura, S. Ishihara, S. Maekawa, and Y. Tokura, *Nature* **410**, 180 (2001).

⁶ S. Nakatsuji and Y. Maeno, *Phys. Rev. Lett.* **84**, 2666 (2000).

⁷ S. Nakatsuji and Y. Maeno, *Phys. Rev. B* **62**, 6458 (2000).

⁸ O. Friedt, M. Braden, G. André, P. Adelmann, S. Nakatsuji, and Y. Maeno, *Phys. Rev. B* **63**, 174432 (2001).

⁹ Y. Maeno, H. Hashimoto, K. Yoshida, S. Nishizaki, T. Fujita, J. G. Bednorz, and F. Lichtenberg, *Nature (London)* **372**, 532 (1994).

¹⁰ K. Ishida, H. Mukuda, Y. Kitaoka, K. Asayama, Z. Q. Mao, Y. Mori, and Y. Maeno, *Nature (London)* **396**, 658 (1998).

¹¹ J. A. Duffy, S. M. Hayden, Y. Maeno, Z. Mao, J. Kulda, and G. J. McIntyre, *Phys. Rev. Lett.* **85**, 5412 (2000).

¹² S. Nakatsuji, S. Ikeda, and Y. Maeno, *J. Phys. Soc. Jpn.* **66**, 1868 (1997).

¹³ S. Nakatsuji, D. Hall, L. Balicas, Z. Fisk, K. Sugahara, M. Yoshioka, and Y. Maeno, *Phys. Rev. Lett.* **90**, 137202 (2003).

¹⁴ J. S. Lee, Y. S. Lee, T. W. Noh, S.-J. Oh, J. Yu, S. Nakatsuji, H. Fukazawa, and Y. Maeno, *Phys. Rev. Lett.* **89**, 257402 (2002).

- ¹⁵ R. Jin, J. R. Thompson, J. He, J. M. Farmer, N. Lowhorn, G. A. Lamberton, Jr., T. M. Tritt, and D. Mandrus, *cond-mat/0112405*.
- ¹⁶ J. Schoenes and J. J. M. Franse, *Phys. Rev. B* **33**, 5138 (1986).
- ¹⁷ V. I. Anisimov, I. A. Nekrasov, D. E. Kondakov, T. M. Rice, and M. Sigrist, *Eur. Phys. J. B* **25**, 191 (2002).
- ¹⁸ A. Koga, N. Kawakami, T. M. Rice, and M. Sigrist, *Phys. Rev. Lett.* **92**, 216402 (2004).
- ¹⁹ A. Liebsch and H. Ishida, *Phys. Rev. Lett.* **98**, 216403 (2007).
- ²⁰ S.-C. Wang, H.-B. Yang, A. K. P. Sekharan, S. Souma, H. Matsui, T. Sato, T. Takahashi, C. Lu, J. Zhang, R. Jin, D. Mandrus, E. W. Plummer, Z. Wang, and H. Ding, *Phys. Rev. Lett.* **93**, 177007 (2004).
- ²¹ Z. Fang and K. Terakura, *Phys. Rev. B* **64**, 020509(R) (2001).
- ²² M. C. Gutzwiller, *Phys. Rev. Lett.* **10**, 159 (1963); *Phys. Rev.* **137**, A1726 (1965).
- ²³ T. Ogawa, K. Kanda, and T. Matsubara, *Prog. Theor. Phys.* **53**, 614 (1975).
- ²⁴ P. Fazekas, *Lecture Notes on Electron Correlation and Magnetism* (World Scientific, Singapore, 1999).
- ²⁵ J. Bünemann, W. Weber, and F. Gebhard, *Phys. Rev. B* **57**, 6896 (1998).
- ²⁶ M. Ogata and A. Himeda, *J. Phys. Soc. Jpn.* **72**, 374 (2003).
- ²⁷ T. Oguchi, *Phys. Rev. B* **51**, 1385 (1995).
- ²⁸ D. J. Singh, *Phys. Rev. B* **52**, 1358 (1995).
- ²⁹ H.-J. Noh, S.-J. Oh, B.-G. Park, J.-H. Park, J.-Y. Kim, H.-D. Kim, T. Mizokawa, L. H. Tjeng, H.-J. Lin, C. T. Chen, S. Schuppler, S. Nakatsuji, H. Fukazawa, and Y. Maeno, *Phys. Rev. B* **72**, 052411 (2005).
- ³⁰ S. J. Moon, M. W. Kim, K. W. Kim, Y. S. Lee, J.-Y. Kim, J.-H. Park, B. J. Kim, S.-J. Oh, S. Nakatsuji, Y. Maeno, I. Nagai, S. I. Ikeda, G. Cao, and T. W. Noh, *Phys. Rev. B* **74**, 113104 (2006).
- ³¹ Y. Yanase and M. Ogata, *J. Phys. Soc. Jpn.* **72**, 673 (2003).
- ³² A. P. Mackenzie, S. R. Julian, A. J. Diver, G. J. McMullan, M. P. Ray, G. G. Lonzarich, Y. Maeno, S. Nishizaki, and T. Fujita, *Phys. Rev. Lett.* **76**, 3786 (1996).
- ³³ T. Oguchi, *J. Phys. Soc. Jpn.* **78**, 044702 (2009).
- ³⁴ W. H. Press, S. A. Teukolsky, W. T. Vetterling, and B. P. Flannery, *NUMERICAL RECIPES* (Cambridge University Press, New York, 2007).
- ³⁵ A. Georges and W. Krauth, *Phys. Rev. B* **48**, 7167 (1993).
- ³⁶ N. Furukawa and M. Imada, *J. Phys. Soc. Jpn.* **62**, 2557 (1993).
- ³⁷ H. Yokoyama and H. Shiba, *J. Phys. Soc. Jpn.* **59**, 3669 (1990).
- ³⁸ H. Yokoyama, *Prog. Theor. Phys.* **108**, (2002) 59.
- ³⁹ H. Yokoyama, Y. Tanaka, M. Ogata, and H. Tsuchiura, *J. Phys. Soc. Jpn.* **73**, 1119 (2004).
- ⁴⁰ H. Yokoyama, M. Ogata, and Y. Tanaka, *J. Phys. Soc. Jpn.* **75**, 114706 (2006).
- ⁴¹ H. Yokoyama, M. Ogata, Y. Tanaka, K. Kobayashi, and H. Tsuchiura, in preparation.
- ⁴² K. Haule and G. Kotliar, *New J. Phys.* **11**, 025021 (2009).
- ⁴³ J. Mravlje, M. Aichhorn, T. Miyake, K. Haule, G. Kotliar, and A. Georges, *Phys. Rev. Lett.* **106**, 096401 (2011).
- ⁴⁴ L. de' Medici, J. Mravlje, and A. Georges, *Phys. Rev. Lett.* **107**, 256401 (2011).
- ⁴⁵ Y. Yoshioka and K. Miyake, *J. Phys. Soc. Jpn.* **78**, 074701 (2009).
- ⁴⁶ E. Ko, B. J. Kim, C. Kim, and H. J. Choi, *Phys. Rev. Lett.* **98**, 226401 (2007).
- ⁴⁷ A. Gukasov, M. Braden, R. J. Papoular, S. Nakatsuji, and Y. Maeno, *Phys. Rev. Lett.* **89**, 087202 (2002).
- ⁴⁸ G. Cao, S. McCall, M. Shepard, J. E. Crow, and R. P. Guertin, *Phys. Rev. B* **56**, 321 (1997).
- ⁴⁹ N. Kikugawa, A. P. Mackenzie, C. Bergemann, R. A. Borzi, S. A. Grigera, and Y. Maeno, *Phys. Rev. B* **70**, 060508(R) (2004).
- ⁵⁰ N. Kikugawa, C. Bergemann, A. P. Mackenzie, and Y. Maeno, *Phys. Rev. B* **70**, 134520 (2004).
- ⁵¹ K. M. Shen, N. Kikugawa, C. Bergemann, L. Balicas, F. Baumberger, W. Meevasana, N. J. C. Ingle, Y. Maeno, Z.-X. Shen, and A. P. Mackenzie, *Phys. Rev. Lett.* **99**, 187001 (2007).
- ⁵² T. Moriya and A. Kawabata, *J. Phys. Soc. Jpn.* **34**, 639 (1973).
- ⁵³ N. F. Berk and J. R. Schrieffer, *Phys. Rev. Lett.* **17**, 433 (1966).
- ⁵⁴ S. Doniach and S. Engelsberg, *Phys. Rev. Lett.* **17**, 750 (1966).
- ⁵⁵ O. Friedt, P. Steffens, M. Braden, Y. Sidis, S. Nakatsuji, and Y. Maeno, *Phys. Rev. Lett.* **93**, 147404 (2004).
- ⁵⁶ T. Moriya and T. Takimoto, *J. Phys. Soc. Jpn.* **64**, 960 (1995).
- ⁵⁷ Y. Maeno, K. Yoshida, H. Hashimoto, S. Nishizaki, S. Ikeda, M. Nohara, T. Fujita, A. P. Mackenzie, N. E. Hussey, J. G. Bednorz, and F. Lichtenberg, *J. Phys. Soc. Jpn.* **66**, 1405 (1997).